People's Democratic Republic of Algeria
Ministry of Higher Education and Scientific Research

University M'Hamed BOUGARA – Boumerdes

Institute of Electrical and Electronic Engineering

Department of Power and Control

Final Year Project Report Presented in Partial Fulfilment of the Requirements for the Degree of

MASTER

In **Power Engineering**

Option: **Power Engineering**

Title:

Design and implementation of T-type three level inverter based grid-connected PV system

Presented by:

- **MERAZKA Abdeslam**
- **LAZOUECHE Youssouf**

Supervisor:

Dr. KHELDOUN Aissa

Registration Number:……/2018

Dedication

Every challenging work needs self-efforts as well as guidance of Elders those who were very close to our heart.

My humble effort I dedicate to my sweet and loving

***Mother** and my **family members**,*

Whose affection, love, encouragement and prays of day and night make me able to get such success and honor.

*Along with all **my friends**, **hardworking** and respected **Teachers** and a special dedication to **2013 promotion** especially **POWER option.***

Abdeslam MERAZKA.

Dedication from LAZOUECHE YOUSSOUF:

I dedicate this work to my dear dad and beloved mom, to my brothers, sisters and to all my friends and also special dedication to 2013 promotion without forgetting the people who helped me and encouraged me until I reached this point today, from near or from far.

Acknowledgment

First and foremost, we would like to thank ALLAH the almighty, for giving us the strength, knowledge and the ability to undertake this project study and complete it satisfactorily. Without his blessings, this achievement would not have been possible.

We would like to express our deepest sense of gratitude to the supervisor Dr. **KHELDOUN Aissa** for his guidance, support and help throughout the different phases of the project. And to all and every teacher who taught and guide us from primary school to the last year of study.

Abstract

Due to its intermittence, strong dependability on the climate conditions, penetration of PV plants to grid utilities is a big challenge for the power system operators. This project is intended to design and implement a three-phase grid-connected PV system. Two controllers will be developed namely the Golden Section Search (GSS) –based MPPT and the SVM for the three level T-type inverter being used as interface with the Gird. The MPPT algorithm ensures maximum power extraction from the PV generator and the SVM ensures the requirements of grid connection standard in terms of power quality.

Phase locked loop (PLL) is used to lock the grid phase and frequency and to eliminate the high frequency ripples and reduce the THD at the inverter output an LCL filter is used.

Table of Contents

Chapter one: Modeling of PV system

Chapter two: Modeling of Three-level inverter

Chapter three: Design of Grid connected PV system

Chapter Four: Simulation and Implementation

List of Figures

List of Tables

Acronyms

DC Direct current.
AC Alternating current.
PV Photovoltaic.
I Current.
V Voltage.
I_L Light generated current.
I_O Saturation Current.
Rs Series Resistance.
A Diode ideality factor.
k Boltzmann's constant.
q Charge on an electron.
T_C Working cell Temperature.
Isc Short circuit current.
T_{ref} Reference Temperature.
G Irradiance [W/m²].
I_{RS} Reveres saturation current.
E_G Band-gap energy.
Voc Open Circuit Voltage.
P_{max} Maximum power.
P-V Power-Voltage.
FF Fill Factor.
η Efficiency.
I_{ph} Photocurrent.
I_{mp} Current at maximum power.
V_{mp} Voltage at maximum power.
PCU Power Conditioning Unit.
MPPT Maximum Power Point Tracking.
MPP Maximum Power Point.
MLI Multi Level Inverter.
THD Total Harmonic Distortion.
NPC Neutral Point Clamped.
IGBT Isolated Gate Bipolar Transsistor.
lEGT Injection Enhanced Gate Transistor.
PWM Pulse Width Modulation.
NP Neutral Point.
IPD In-Phase Disposition.
APOD Alternative Phase Opposition Disposition.
POD Phase Opposition Disposition.

SVM	Space Vector Modulation.
PLL	Phase-Locked Loop.
SVPWM	Space Vector Pulse Width Modulation.
PI	Proportional-Integrator.
GSS	Golden Section Search.
P&O	Perturb and Observe.
VOC	Voltage Oriented Control.
VSI	Voltage Source Inverter.
P	Power.
RMS	Root Mean Square.
FFT	Fast Fourier Transform.
PF	Power Factor.
Hz	Hertz.
PCB	Printed Circuit Board.

General Introduction

Due to the great dependability to fossils in energy production all around the world and its huge effect on ecology and economy, the tendency to use more reliable and renewable energy sources is growing remarkably.

PV energy is one of the biggest promising energy sources with very huge availability and practically zero pollution, however its main drawback is its low efficiency and complicated controlling technique at an expensive cost, for that lot of researches have been carried out to maximize the system efficiency and simplify its design and controlling techniques.

Among variety of types of PV systems, the grid connected PV system is considered the best solution to assure the continuity of power and minimize cost. PV systems depends on PV effect to converts solar energy into a DC power, for that the use of inverters is essential to perform the DC/AC conversion, on the other hand to improve the PV system efficiency lot of maximum power point tracking algorithms (MPPTs) were developed.

This modest work goes in the details of the design and implementation of T-type three level inverter based grid connected PV system with single stage maximum power point tracking capability. The report is divided into 4 chapters: chapter one deals with the modeling and principal of working of PV system, whereas chapter two is devoted to present in details the key element of the PV system that is the three level inverter. Chapter three gives a clear idea about the design of grid connected PV system and in chapter four the simulation and part of the implementation is presented.

Finally, some recommendations for further work are stated to improve the system capabilities.

Chapter One

Modeling of PV system

1.1 Introduction

With the increasing demand on power all around the world and even the pollution problems, the need for new energy sources that are renewable and pure becomes more and more interesting. One of the solutions is solar or as it is called Photovoltaic energy.

From its name, Photovoltaic systems use photovoltaic effect to convert sunlight into electricity that is the most known way of using solar energy. According to Einstein law E=h*ν, the electromagnetic radiation of sunlight can be directly converted into direct electricity, through the effect of photovoltaic, however the conversion of solar energy passes through many phases and require complicated controlling loops to reach the form of a useful energy.

Depending on the application, comprises batteries for electricity storage, DC/AC inverters that connect a PV solar system to the electrical grid, and other miscellaneous electrical components or mounting elements are essential in a PV system.
This chapter goes in details about modeling and principle of working of a PV system.

1.2 Solar radiation

The basic processes behind the photovoltaic effect, on which the operation of solar cells is based, is generation of the electron-hole pairs due to absorption of visible or other electromagnetic radiation by a semiconductor material. Today we accept that electromagnetic radiation can be described in terms of waves, which are characterized by wavelength (λ) and frequency (ν), or in terms of discrete particles, ***photons***, which are characterized by energy (*h*ν*) expressed in electron volts. The following formulas show the relations between these quantities:

$$\nu = c / \lambda \tag{1.1}$$

$$E = h\nu = \frac{1}{q}\frac{hc}{\lambda} \tag{1.2}$$

Where **c** is the speed of light in vacuum (2.998×10^8 m/s), **h** is Planck's constant (6.625×10^{34} Js), and **q** is the elementary charge (1.602×10^{19} C).

Only photons of appropriate energy can be absorbed and generate the electron-hole pairs in the semiconductor material, more specifically only photons that have energy equal or greater than the band gap energy of the electron are able to make that

latter free and create the electron-hole pair. Therefore, it is important to know the spectral distribution of the solar radiation [2].

1.3 Solar Cell

The basic building block of PV technology is the photovoltaic cell. Different materials are used to produce PV cells, but silicon is the main ingredient since it is mainly extracted from sand, which by itself is widely available.

Solar cell is merely a p-n junction semiconductor device; the p-n junction (diode) is a boundary between two differently doped semiconductor layers, one is a P-type layer (excess holes), and the other is an N-type (excess electrons). At the boundary between the P and the N area there is a spontaneous electric field, which affects the generated electrons and holes and determines the direction of the current [1].

1.3.1 Solar cell working principle

To obtain the energy by the photovoltaic effect, there shall be a directed motion of photoelectrons, i.e. electricity. All charged particles, photoelectrons also, move in a directed motion under the influence of electric field. The electric field in the material itself is located in semiconductors, precisely in the impoverished area of PV junction (diode).

It was pointed out for the semiconductors that, along with the free electrons in them, there are holes (also called cavities) as charge carriers, which are a sort of a byproduct in the emergence of free electrons. Holes occurs whenever the valence electron turns into a free electron, and this process is called the generation, while the reverse process, when the free electron fills the empty space and combine with a hole, is called recombination. If the electron-hole pairs occur away from the impoverished areas, it is possible to recombine before they are separated by the electric field.

Electrons and holes in semiconductors are accumulated at opposite ends, thereby creating an electromotive force. If a consuming device is connected to such a system, the current will flow and we will get electricity.

In this way, solar cells produce a voltage around 0.5-0.7 V, with a current density of about several tens of mA/cm^2 depending on the solar radiation power as well as on the radiation spectrum [1].

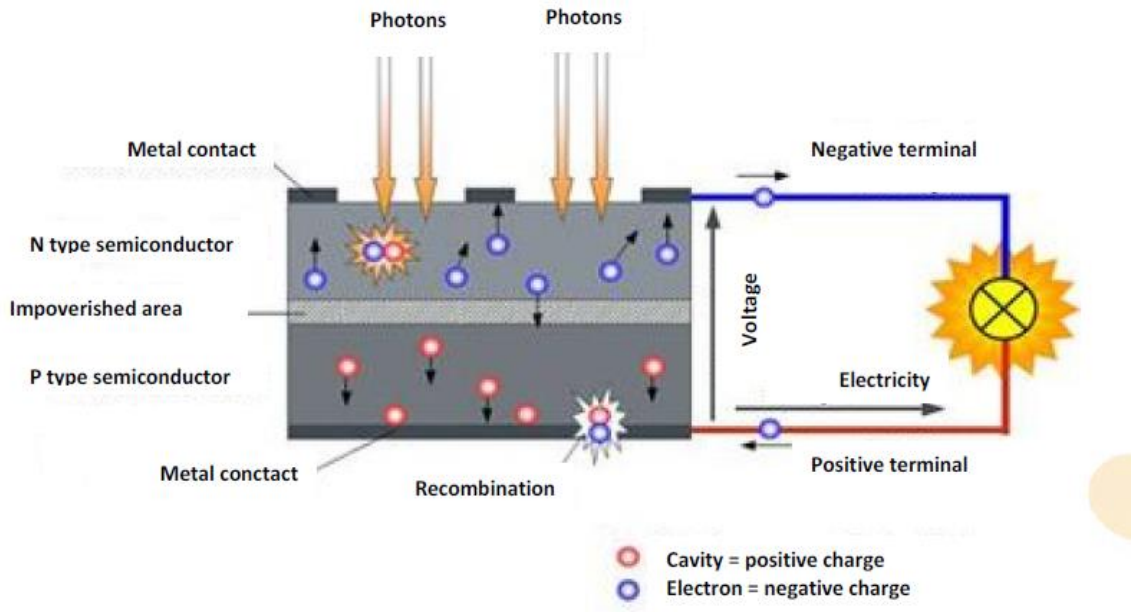

Figure 1.1 Functioning of the photovoltaic cell [1].

1.3.2 Equivalent circuit of photovoltaic cell

Several circuits can model solar cell, the equivalent circuit of an ideal cell is formed by a current source in parallel with a diode. Several circuits include resistors for real effects of a photovoltaic cell. Other models include two diodes. However the model of figure 1.2 is the most commonly used.

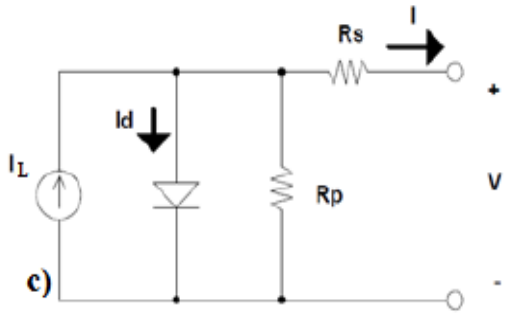

Figure 1.2 Equivalent circuits of photovoltaic cell.

1.3.3 Mathematical modeling of a photovoltaic cell

The most common model used to predict energy production in photovoltaic cell modeling is the single diode circuit model (figure 1.2.c) that represents the electrical behavior of the pn- junction. Therefor the I-V characteristics equation of solar cell is given as follows:

$$I = I_L - I_O\{e^{[\frac{q(V+IRs)}{AkT_c}]} - 1\} - \frac{(V+IRs)}{R_P} \quad (1.3)$$

I_L is a light generated current or photocurrent (representing the current source), I_O is the saturation current (representing the diode), Rs series resistance, A is diode ideality factor, k (= 1.38 $\times 10^{23}$ W/m^{2}K) is Boltzmann's constant, q (=1.6$\times 10^{19}$C) is the magnitude of charge on an electron and T_C is working cell temperature.

Such that:

$$I_L = G[I_{SC} + K_I(T_C - T_{ref})] \quad (1.4)$$

Where Isc is the short circuit current at 25℃ and 1KW/m^2, K_I is the short circuit current temperature coefficient, T_{ref} is the reference temperature and G is the solar insolation KW/m^2.

On the other hand, the cells diode current or saturation current varies with the cell temperature that is described as:

$$I_O = I_{RS}(\frac{T_C}{T_{ref}})^3 e^{[\frac{qE_G(\frac{1}{Tref} * \frac{1}{Tc})}{Ak}]} \quad (1.5)$$

Where I_{RS} is the cells reveres saturation current at reference temperature and a solar radiation E_G is the band-gap energy of the semiconductor used in cell [2].

1.3.4 I-V and P-V Curves of PV system

The I-V (current-voltage) curve of a PV string (or module) describes its energy conversion capability at the existing conditions of irradiance (light level) and temperature.

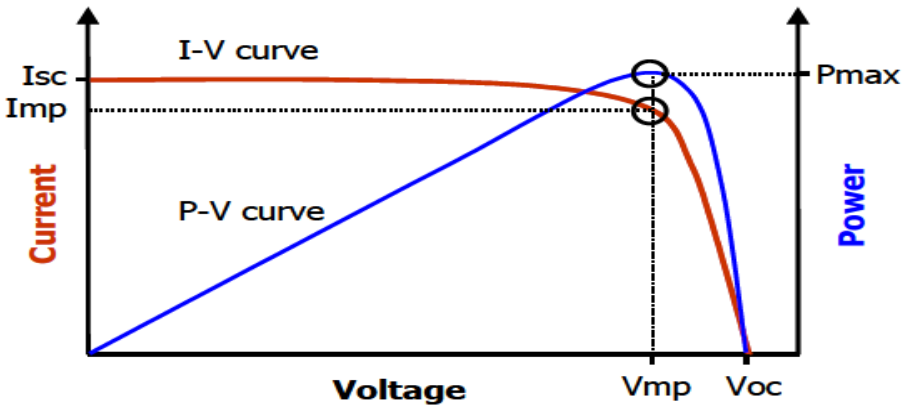

Figure 1.3 The I-V and P-V curves of a photovoltaic device [5].

Referring to Figure 1.3, the span of the I-V curve ranges from the short circuit current (Isc) at zero volts, to zero current at the open circuit voltage (Voc). At the 'knee' of a normal I-V curve is the maximum power point (Imp, Vmp), the point at which the array generates maximum electrical power. In an operating PV system, one of the jobs of the inverter is to constantly adjust the load, seeking out the particular point on the I-V curve at which the array as a whole yields the greatest DC power.

The I-V curve of a PV cell, module, or array does not by itself tell us anything about just where on that curve the system will actually be operating. This determination is a function of the load into which the PV delivers its power.

•Loads do have their own I-V curves: The same voltage is across both the PV and load, and the same current runs through the PV and load.

•The intersection point of the two curves is the operating point.

Plotting equation (1.3) will lead to the following curve that clarifies the PV cell behavior [4]:

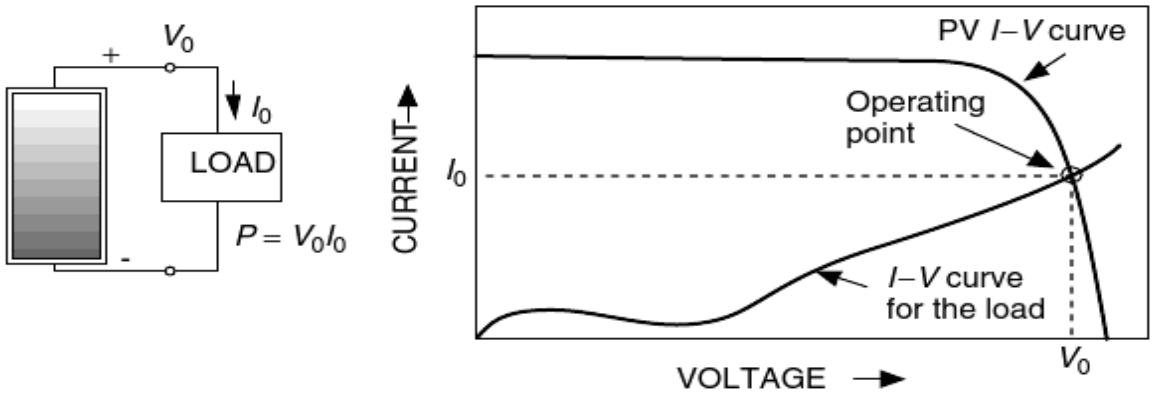

Figure 1.4 I-V Curve for Different loads [4].

- **Scaling I-V curves**

Thinking of PV arrays as composites of smaller PV building blocks is key to interpreting electrical measurements in troubleshooting situations. The I-V curve of a PV array is a scale-up of the I-V curve of a single cell, as illustrated in Figure 1.5.

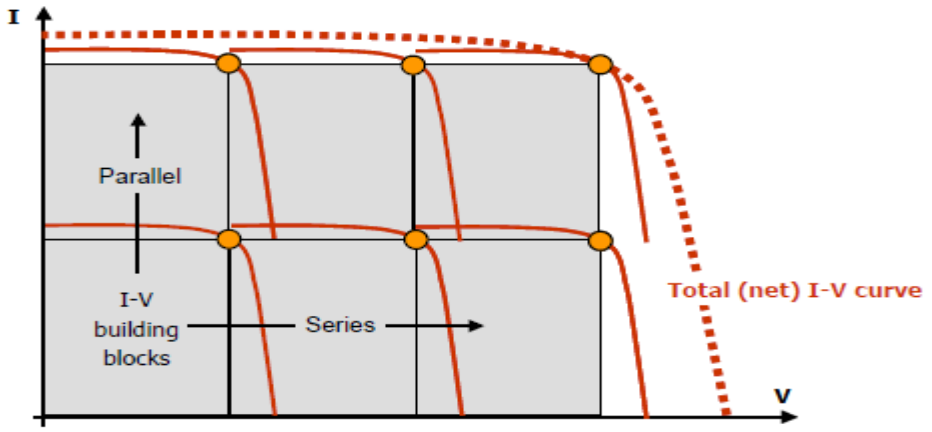

Figure 1.5 Scaling the I-V curve from a PV cell to a PV array [5].

- **Shading Effects**

In a PV module, all the cells are connected in series, thus the same current must flow through each cell. The shaded cells operate at a current higher than their short-circuit current which occurs at negative voltage, thus yielding negative power. The shaded cells will dissipate power as heat and cause "hot spots." Bypass diodes allow current to pass around shaded cells thereby reducing the voltage losses of the system [5].

1.3.5 Solar cell external parameters

- **Short-circuit current**

The short-circuit current, Isc, is the current that flows through the external circuit when the electrodes of the solar cell are short-circuited. It depends on the photon flux density incident on the solar cell that is determined by the spectrum of the incident light [5].

- **Open-circuit voltage**

The open-circuit voltage is the maximum voltage that a solar cell can deliver at which no current flows through the external circuit.

$$V_{OC} = \frac{kT}{q} \ln\left(\frac{I_{ph}}{I_O} + 1\right) \qquad (1.6)$$

Where I_{ph} is the photocurrent and can be approximated by equation (1.7). In the ideal case, Isc is equal to the I_{ph}.

$$I_{ph} = qG(L_N + W + L_P) \qquad (1.7)$$

- **Fill factor**

The fill factor is the ratio between the maximum power ($Pmax = Imp \times Vmp$) generated by a solar cell and the product of Voc and Isc. In other words, it is the ratio of two areas defined by the I-V curve, as illustrated in Figure 1.6 (a).

$$FF = \frac{I_{mp}V_{mp}}{I_{sc}V_{oc}} \tag{1.8}$$

Any impairment that reduces the fill factor also reduces the output power by reducing Imp or Vmp or both. The I-V curve itself helps us identify the nature of these impairments. The effects of series losses, shunt losses and mismatch losses on the I-V curve are represented in Figure 1.6 (b).

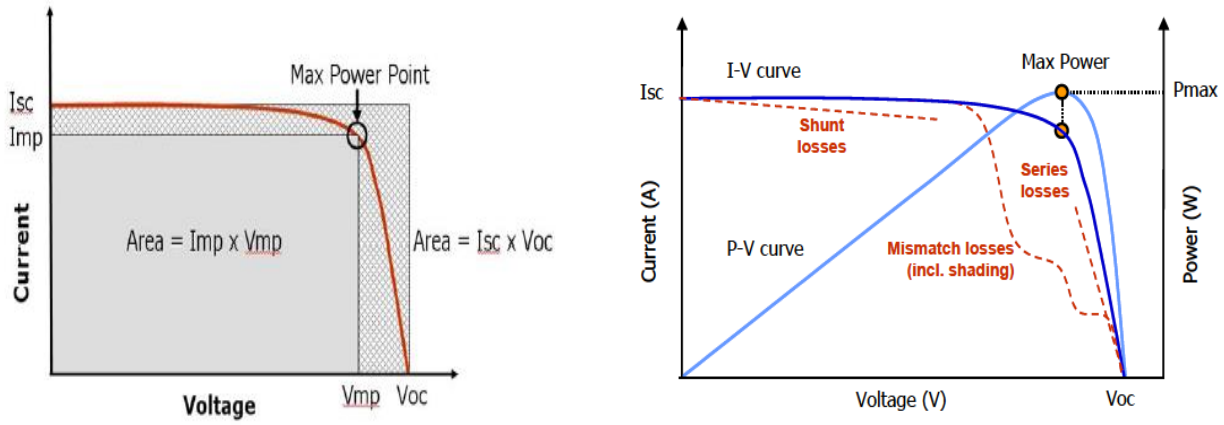

(a) **(b)**

Figure 1.6 (a) The Fill Factor, defined as the gray area divided by the cross-hatched area. **(b)** Several categories of losses that can reduce PV array output [5].

- **Conversion efficiency**

The conversion efficiency is calculated as the ratio between the generated maximum power and the incident power.

$$\eta = \frac{P_{max}}{P_{in}} = \frac{I_{mp}V_{mp}}{P_{in}} = \frac{I_{sc}V_{oc}FF}{P_{in}} \tag{1.9}$$

1.3.6 Types of solar photovoltaic cells

The main types of a solar are:

• **Monocrystalline**, conversion efficiency for this type of cells ranges from 13% to 17% and the expected lifespan of these cells is typically 25-30 years.

• **Polycrystalline**, more efficient compared to monocrystalline, the lifespan is expected to be between 20 and 25 years.

• **Thin-film technology**, lower efficiency ranges from 5% to 13% with lifespan around 15-20 years. Although less efficient than mono and polycrystalline silicon, thin-film solar cells offer greater promise for large-scale power generation because of ease of mass-production and lower materials cost [1].

1.4 Solar module

The power produced by a PV cell is very small, for that, many PV cells are connected in series or parallel to form solar modules. However, the power produced by a single module still not enough for commercial use, so modules are connected to form array to supply the load.

1.5 Solar array

For large-scale generation of solar electricity the solar panels are connected together in series and parallel to comprise the solar array according the demands.

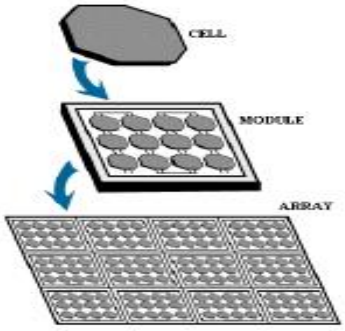

Figure 1.7 Solar PV Cell, Module and Array [2].

1.6 Photovoltaic system types

Photovoltaic power systems are generally classified according to their functional and operational requirements, their component configurations, and how the equipment is connected to other power sources and electrical loads, this section will state the most common types of a PV system.

1.6.1 Grid connected systems (on-grid)

Grid-connected or utility-interactive PV systems are designed to operate in parallel with the electric utility grid. The main components of a grid connected PV

system are PV modules, inverter, mounting sub-frame and measuring cabinet with protective equipment and installation.

PV modules convert solar energy into DC current, while the inverter that is the primary component of the power conditioning unit (PCU), adjusts the produced energy in a form that can be submitted to the public grid by converting the DC power produced by the PV array into AC power consistent with the voltage and power quality requirements of the utility grid. Moreover the PCU automatically stops supplying power to the grid when the utility grid is down for maintenance or during grid failure state. Finally, the AC voltage is supplied to the electricity network through the protection and measuring equipment.

A bi-directional interface can be made between the PV system AC output circuits and the electric utility network. This allows the AC power produced by the PV system to either supply on-site electrical loads or to back-feed the grid when the PV system output is greater than the on-site load demand.

Figure 1.8 shows the general block diagram of the grid connected PV system.

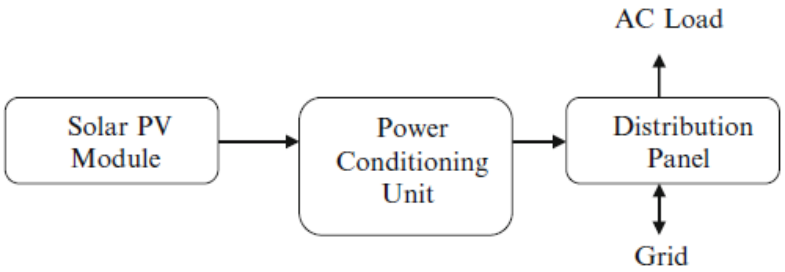

Figure 1.8 Block diagram of grid-connected solar PV system.

1.6.2 Stand-alone systems (off-grid)

Such systems are used in rural and remote areas where there is no electricity network, it is generally designed and sized to supply certain DC and/or AC electrical loads.

Typical stand-alone PV systems are connected to a reservoir of energy (battery) by a control over the charging and discharging. The inverter can also be used to provide alternating current for standard electrical equipment and appliances.

The simplest type of stand-alone PV system is a direct-coupled system, where the DC output of a PV module or array is directly connected to a DC load. It is called direct coupled systems because the DC output of a PV module or array is directly connected to a DC load. There is no electrical energy storage (batteries), as because of that, the

load only operates during sunlight hours. The maximum power point tracker (MPPT) is used between the array and load to help better utilize the available array maximum power output and for matching the impedance of the electrical load to the maximum power output of the PV array.

Figure 1.9 shows the general block diagram of the stand-alone solar PV system [4].

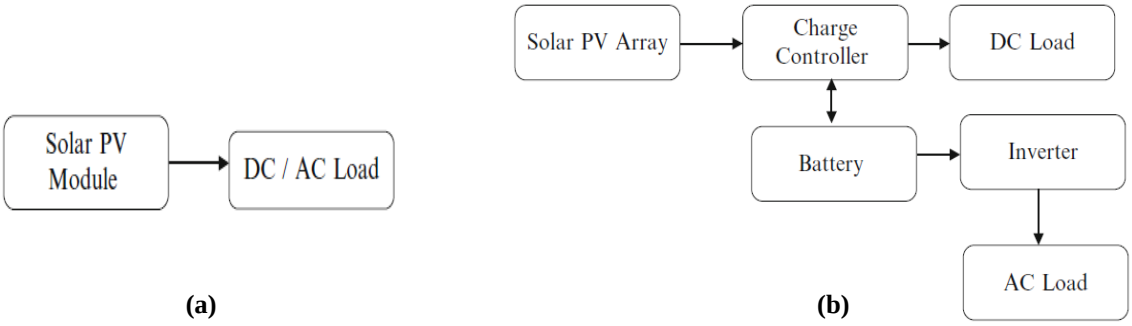

Figure 1.9 (a) Direct coupled solar PV system. **(b)** Block diagram of stand-alone PV system with battery storage.

1.6.3 Hybrid systems

If you were thinking that there is nothing stopping you from having both types of system installed at the same time you would be absolutely right. A Hybrid system gives you all the benefits of both systems with the added benefits of protection from power cuts and outages, coupled with the ability to live independently of fossil fuels while supplying others with clean green energy.

Hybrid systems generally refers to the combination of any two input sources, here solar PV can be integrated with Diesel Generator, Wind Turbines, Bio-mass or any other renewable on non-renewable energy sources. Since it is known that, no renewable energy sources, including photovoltaic systems, are constant in energy production. It means that, when there is no sun, the system does not produce electricity, for that a hybrid PV system takes place to ensure a constant and sufficient supply of electricity. Hybrid systems can also be sensible approach in situations where occasional demand peaks are significantly higher than the base load demand.

A Hybrid Solar PV System would use a connection to the grid enabling power to be exported and use batteries to protect against power cuts and store power for local use.

Please note that, as with all grid connected PV systems, in hybrid systems we need to protect against islanding, this is where the PV system would continue to generate and export power to the grid even if the mains power was unavailable. For

safety, the PV system will disconnect itself from the grid if the mains power is unavailable [4].

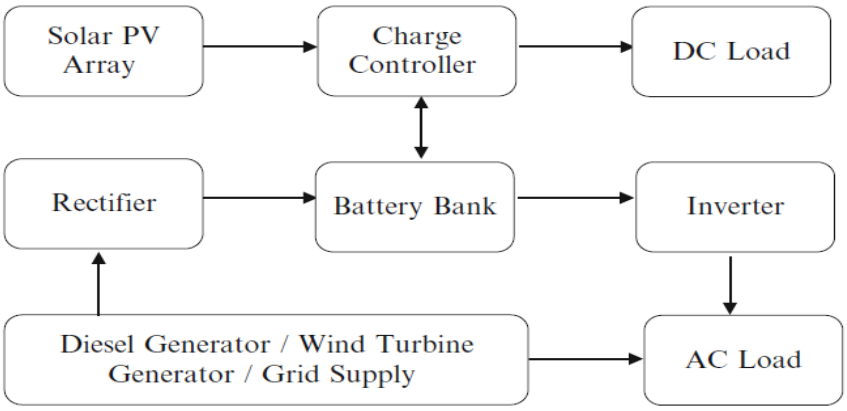

Figure 1.10 Block diagram of photovoltaic hybrid system.

1.7 Advantages and Drawbacks of PV system

The advantages and drawbacks of the PV solar energy can be summarized in the following points:

Advantages:

- No emissions.
- Minimal maintenance requirements.
- Electricity is generated wherever there is light.
- Modular.
- Long lifetime, up to 30 years.
- No noise, no moving parts.

Drawbacks:

- No electric power when there is no light.
- High initial costs.
- Large area needed for large scale applications.
- Inverters and energy storage (batteries) are needed in off-grid applications.

1.8 Conclusion

Solar system uses the Photovoltaic effect in the solar cell to convert the light irradiance to a small DC electric power, to lift up the produced power; PV cells are connected in series and in parallel to form a PV module that is transformed to a PV array through another series and parallel connection.

PV generator can operate as grid connected or standalone system. Moreover, it can be coupled with other power sources to assure the continuity of the supplied power.

Chapter Two

Modeling of Three-Level Inverter

2.1 Introduction

The PV panel delivers a DC power, however most of the loads needs AC power to operate, for that, the inverter plays the role of the key element of grid-connected PV systems. Its main function is to convert the DC power generated by PV panels into grid-synchronized AC one.

Among various kinds of multilevel inverters, the three-level T-type inverter , has drawn a lot of attention these days since it combines the advantages of the two-level inverters such as low conduction losses and a simple operation principle with the positive aspects of three-level inverters such as low switching losses and superior output voltage quality, etc.

For that, this chapter it devoted to give a clear idea about the three-level T-type inverter, its principle of working and the controlling techniques that can be used.

2.2 Types of multi-level inverters

Inverters can be classified according to their level of conversion from two, three to n level inverter. The higher the level the better the power quality and the more expensive and complicated design circuit and control technique, an optimal solution between cost, complexity and power quality is the three level inverter.

Recently, 2-level inverters were replaced by MLIs due to the low level THD and high efficiency output of the latter.

2.2.1 Neutral Point Clamped Inverter

A simplified configuration of a three-level neutral point clamped (NPC) inverter fed drive is shown in Figure 2.1. Some manufacturers use GCTs as switching devices while others use IGBTs or injection enhanced gate transistors (lEGT) in the inverter. The DC link capacitors split the DC voltage into two, providing a neutral point *N.* The diodes connected to the neutral point are referred to as clamping diodes, which clamp the inverter terminal voltage to the neutral point potential. Due to the clamping function of the diodes, the maximum voltage on each of the switches is *E,* which is half of the dc link voltage for the three-level inverter.

Depending on the drive system design requirements, it is optional to use one or two DC voltage sources. With two DC voltage sources, the DC capacitor voltage

is fixed. Otherwise, the DC capacitor voltage is floating, and certain measures should be in place to minimize the neutral point potential deviation [8].

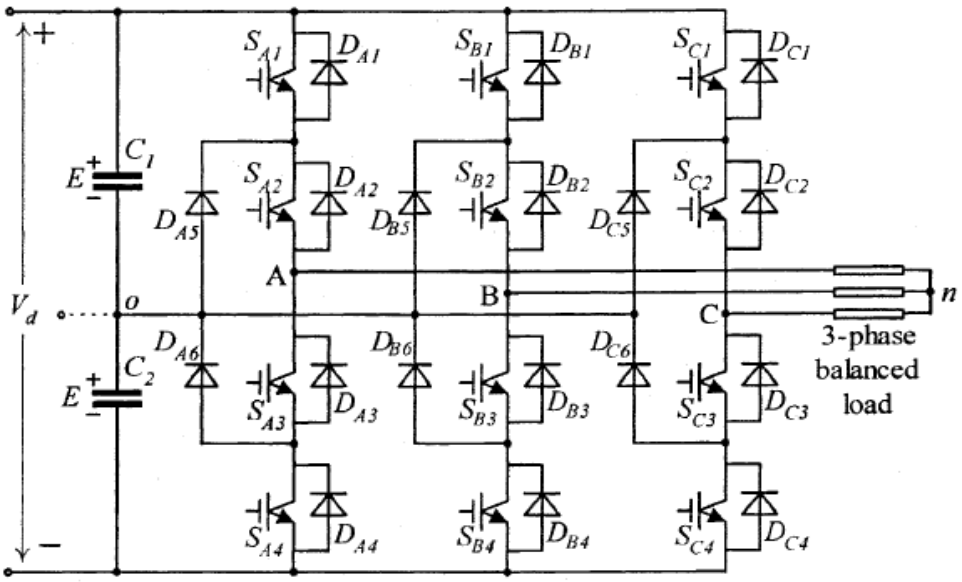

Figure 2.1 Simplified configuration of three-level NPC inverter [8].

The three-level NPC inverter based drive offers the following features and drawbacks:

• **No Dynamic Voltage Sharing Problem.** Mainly due to the use of clamping diodes.

• **Low Harmonics Distortion.** Compared with the conventional two-level inverter, the NPC inverter is able to produce better output voltage waveforms with lower THD.

• **Provision for four-quadrant operation.** For more advanced applications where regeneration capability is necessary, the same topology can be applied to the rectifier working as the DC voltage source.

• **Possible neutral point potential deviation.** Special measures should be taken when designing the PWM schemes to prevent such deviations, which makes the PWM pattern design more complicated.

• **Additional clamping diodes.** The NPC inverter requires clamping diodes. The number of clamping diodes can be calculated by 3(m-l)(m-2), where *m* is the number of voltage levels. The substantial increase in the clamping diodes makes the four-level and five-level inverters impractical for industrial use [8].

2.2.2 Cascaded H-bridge Inverter

Cascaded H-bridge multilevel inverter is one of the popular converter topologies used in megawatt drives. It is composed of multiple units of power cells as shown in

Figure 2.2. Each power cell is mainly composed of an H-bridge inverter powered by a three-phase diode rectifier connected to an isolated secondary winding of a phase shifting (zigzag) transformer.

The power cells in one inverter phase are normally connected in cascade on their ac output side to achieve high voltage operation and low harmonic distortion. The number of power cells in a drive is mainly determined by the operating voltage and manufacturing cost.

The use of identical power cells leads to a modular structure, which is an effective means for cost reduction. The number of voltage levels in a cascaded H-bridge inverter, m, can be found from m = (2H+1), where H is the number of H-bridge cells per phase. The cascaded H-bridge inverters with seven to eleven voltage levels are most widely used in industry.

The multilevel inverter requires a number of isolated DC supplies, each of which feeds a power cell. The dc supplies are normally obtained from multipulse diode rectifiers.

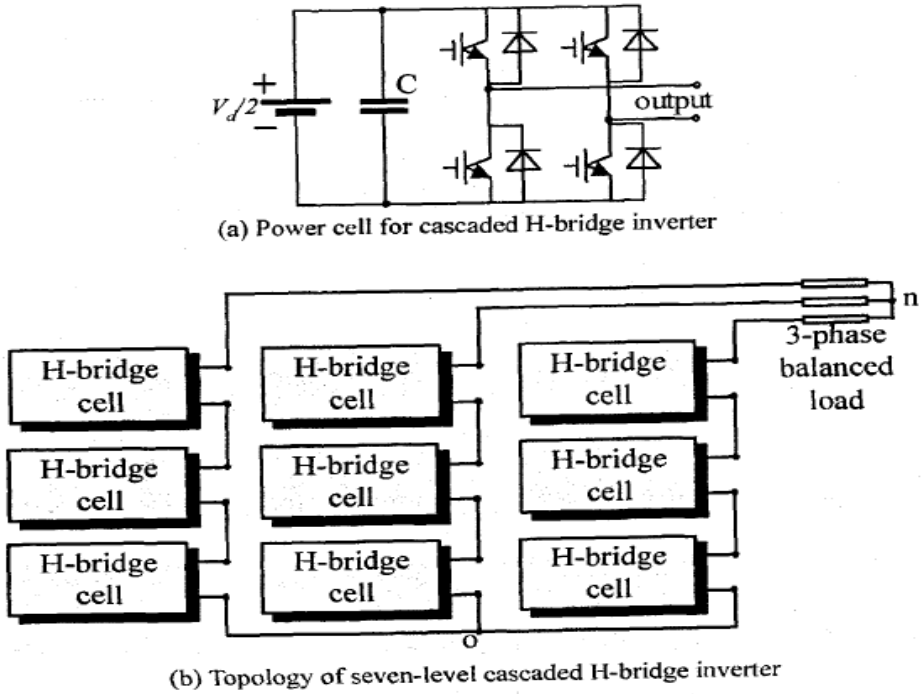

Figure 2.2 Simplified topologies of cascaded H-bridge multilevel inverter [8].

The cascaded H-bridge multilevel inverter fed drive has a number of features, including:

• **Low voltage THD and dv/dt.** The inverter output voltage waveform is formed by several small voltage steps (levels), and distributed sinusoidally over time, resulting in a low THD and dv/dt.

• **Modular structure.** The multilevel inverter is composed of multiple units of identical H-bridge power cells, which is an effective means for reducing the manufacturing cost.

• **High voltage operation without switching devices in series.** The power cells are connected in cascade to withstand high ac voltages. There are no voltage sharing problems among the switching devices.

• **Low line current THD.** The low-order harmonic currents produced by diode rectifiers are cancelled by the phase shifting transformer, assuring compliance with IEEE Standard 519-1992.

• **Optional degrees of redundancy.** The modular nature of the drive allows optional degrees of redundancy.

There are some drawbacks associated with the drive:

• **A large number of isolated dc supplies.** The DC supplies for the cascaded H-bridge inverter are usually obtained from a multipulse diode rectifier employing an expensive phase shifting transformer.

• **No regenerative operation capability.** None of the cascaded H-bridge inverter fed drives currently operating in the field has regenerative operation capability. It is technically possible to design a multilevel regenerative PWM rectifier that provides isolated DC supplies for the inverter. However, the manufacturing cost of such a drive will be too high to be accepted by its user [8].

2.2.3 Flying Capacitor Inverter

As shown in Figure 2.3, the flying-capacitor multilevel inverter can be easily constructed by adding dc capacitors to the two-level inverter. Therefore, it preserves some of the features of the two-level inverter such as modular design. Like other multilevel inverters, the flying-capacitor inverter also features low THD and dv/dt in the inverter output voltage.

The main drawbacks include a) difficulties to balance the voltages on the dc capacitors, b) complex switching pattern design, and c) necessity of isolated pre-charging circuits for the dc capacitors. It is these drawbacks that prevent this topology from a widespread application in high-power drive systems [8].

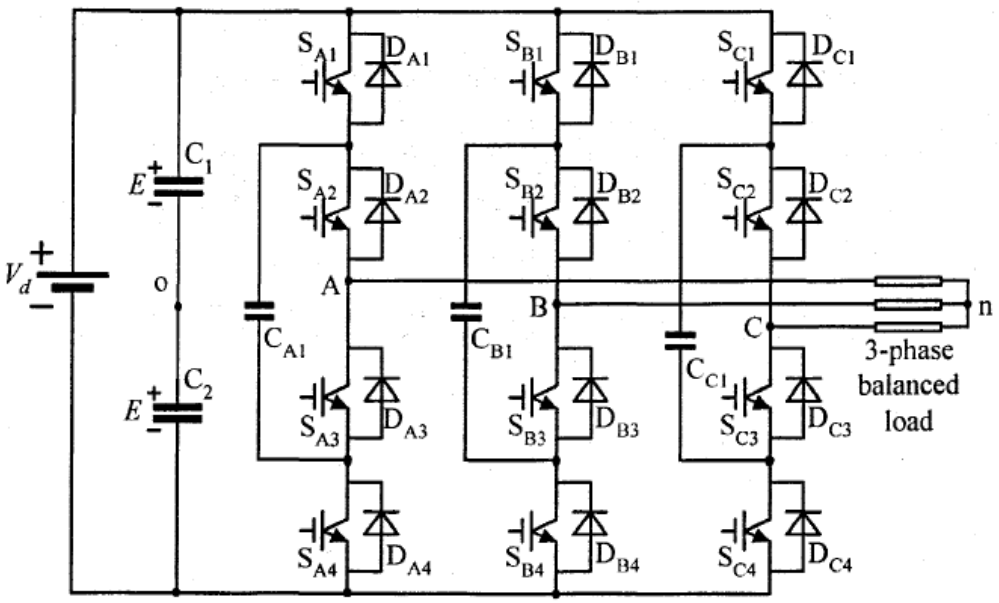

Figure 2.3 Simplified power circuit of three-level flying capacitor inverter [8].

2.2.4 T-type Inverter

T-type converters are becoming popular for low voltage and cost sensitive applications such as for automotive and photovoltaic (PV) converters to achieve high energy conversion efficiency and better power quality. The T-type inverter combines the positive aspects of the two-level inverter such as low conduction losses, small part count and a simple operation principle with the advantages of the three-level inverter mentioned earlier.

Compared to the three-level NPC inverter the T-type inverter employs two active bidirectional switches [see Figure 2.4] to the DC-link voltage neutral point connected back-to-back, thus creating a third output voltage level without the need to the clamping diodes.

As seen, the three-level NPC converter uses two more clamping diodes per leg than the T-type converter, but all the devices just need to withstand half of the dc-link voltage ($V_{dc}/2$). Lower device voltage rating leads to reduced device switching and conduction loss. In the T-type converter, T1(D1), T4(D4) need to withstand the full dc-link voltage (V_{dc}) and T2 (D2) and T3(D3) just needs to withstand half of the dc-link voltage ($V_{dc}/2$). During switching, all the devices in the T-type and NPC converter just need to switch half of the dc-link voltage [3].

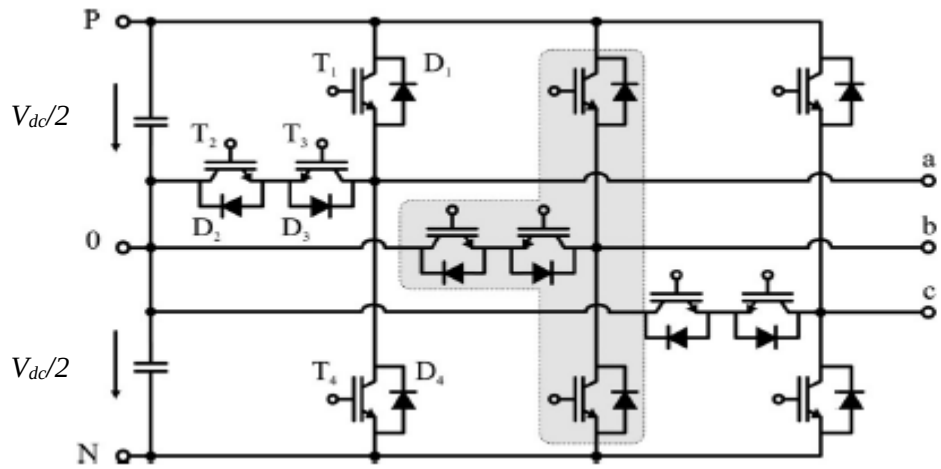

Figure 2.4 Topology of the T-type inverter system [9].

However, a similar to NPC inverter, the major concern for the T-type inverter is the fluctuation in the NP voltage. To take full benefit of this inverter, the neutral-point voltage must be actively balanced. Several researches have been presented to keep the neutral voltage balanced. The analysis is based on selecting redundant vectors in the space-vector diagram for each switching period.

- **Switch Configuration**

There are basically two ways the two clamping switches can be configured to form a bidirectional switch, either in common emitter configuration or in common collector configuration.

The common emitter configuration [see Figure 2.5 (a)] would require one additional isolated gate drive supply voltage for each bridge leg, summing up to three additional gate drive supplies compared to the two-level inverter topology.
This number can be reduced even more if a common collector configuration [Figure 2.5 (b)] is used.

T2 shares now a common emitter with the high-side switch T1 and can be supplied with the isolated gate drive voltage of T1 . The emitter of the second clamping switch is connected to the midpoint voltage level. If the 3-phase topology is considered, all three IGBTs T3,a,b,c share a common emitter, and therefore only one isolated gate drive supply is necessary. In total, the complete T-type topology can be implemented with only one additional isolated gate drive supply compared to the two-level inverter topology [9].

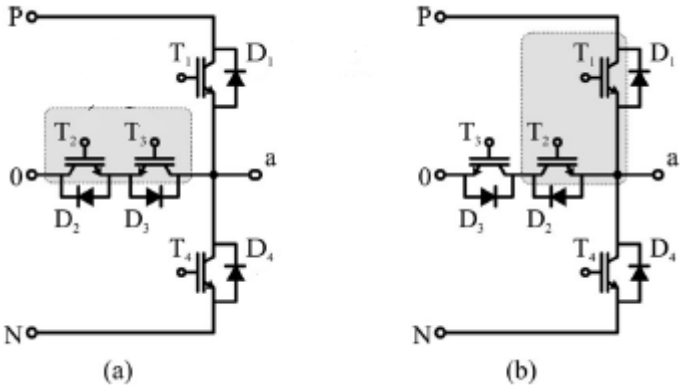

Figure 2.5 Bidirectional switch to the midpoint in **(a)** common emitter configuration, **(b)** common collector configuration [9].

2.3 Modulation Techniques for Multilevel Inverter

The modulation schemes for the multilevel voltage source inverters can be generally classified into carrier based modulation and space vector modulation.

2.3.1 Carrier Based Modulation

There are two commonly-used carrier based modulation schemes: phase-shifted and voltage-shifted modulations. In general, a multilevel inverter with *m* voltage levels requires (m-1) triangular carriers. The modulating signal is usually a three-phase sinusoidal wave with adjustable amplitude and frequency. The gate signals are generated by comparing the modulating wave with the carrier waves.

a) Phase-shifted Modulation

All the triangular carriers of phase-shifted modulation have the same frequency and the same peak-to-peak amplitude, but there is a phase shift between any two adjacent carrier waves, given by $\phi = 360° / (\text{m} - 1)$. Figure 2.6 shows the principle of the phase-shifted modulation for seven-level cascaded H-bridge inverter. The triangular carriers Vcr1 toVcr6 are compared with modulation wave V_{mA} to generate gate signals [8].

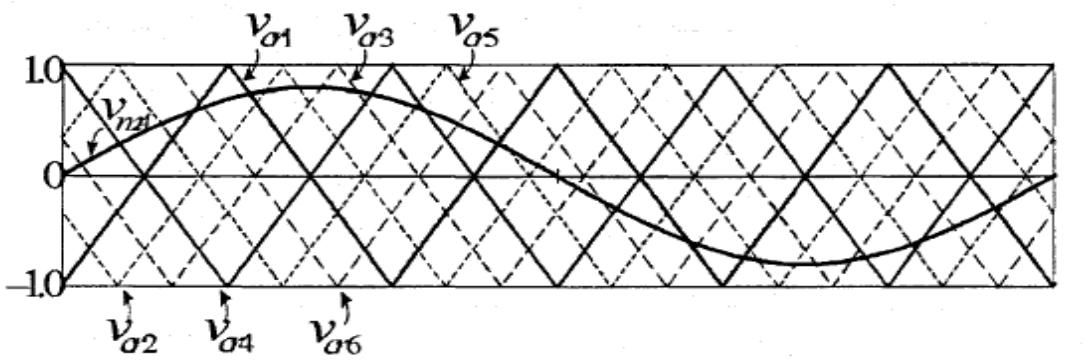

Figure 2.6 Phase-shifted modulation scheme for a seven-level inverter [8].

b) Voltage-shifted Modulation

All of the *(m-1)* triangular carriers of voltage-shifted modulation have the same frequency and amplitude. They are vertically disposed such that the bands they occupy are contiguous. Figure 2.7 shows three schemes for the voltage-shifted modulation for a Five-level inverter: (a) In-Phase Disposition (IPD), where all carriers are in phase; (b) Alternative Phase Opposition Disposition (APOD), where all carriers are alternatively in opposition disposition; and (c) Phase Opposition Disposition (POD), where all carriers above the zero reference are in phase but in opposition with those below the zero reference [8].

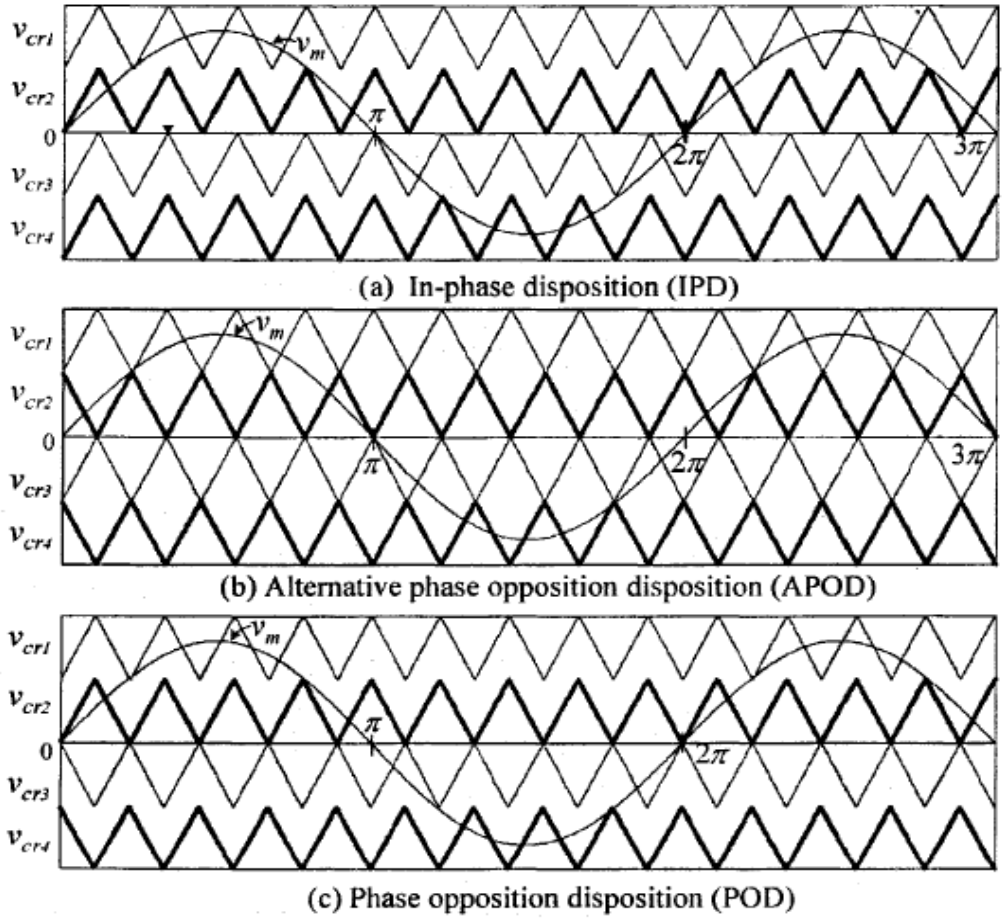

Figure 2.7 Voltage-shifted modulation schemes for a five-level inverter [8].

2.3.2 Space Vector Modulation

Space vector modulation (SVM) is one of the preferred real-time modulation techniques and is widely used for digital control of rectifiers and inverters. For a given inverter (or rectifier) topology, there are a certain number of switching states. Each switching state produces a defined inverter output voltage, which can be represented by stationary voltage vectors in space. A collection of all the space vectors forms a space

vector diagram. A reference voltage vector rotates in space within the space vector diagram. For a given position in space, three nearest stationary vectors can approximate the reference vector on which the gating signals for the switches in the inverter can be generated. Therefore, when the reference vector rotates in space for one revolution, the inverter output voltage changes one fundamental cycle. The magnitude of the inverter fundamental output voltage corresponds to length of the reference vector while its frequency corresponds to the rotating speed of the reference vector and vice versa.
Figure 2.8 shows the space vector diagram for a three-level inverter.

This section presents the general principles of the SVM. The space vectors, reference vector, dwell time calculation, space vector selection and switching state sequence of the inverter [8].

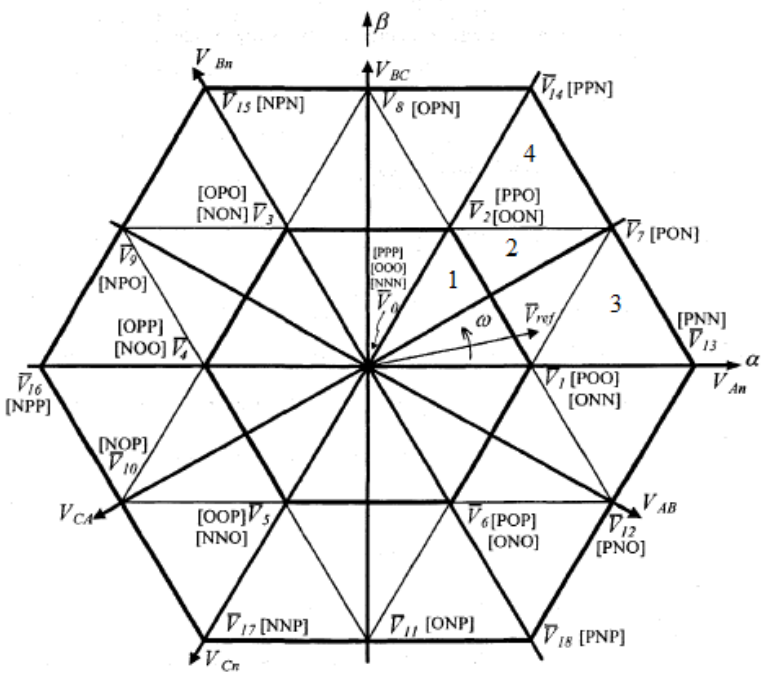

Figure 2.8 Space vectors $(\vec{V}_0 \sim \vec{V}_{18})$ and reference vector $(\vec{V}_{ref})$ for three-level inverters [8].

The space vector modulation in general provides the following features:

- Low harmonics distortion.
- Effective neutral point potential control.
- Easy digital implementation.

However, the traditional space vector modulation scheme produces even order harmonics in the output voltages of the multilevel inverter, which is not desired for most industrial applications. Especially, if SVM scheme is used for three-level

rectifiers, it produces even order harmonics in the input currents, which cannot satisfy the IEEE standards 519-1992 [8].

2.3.2.1 Per-phase Switching States

Each leg in the T-type inverter can take one of three possible states [P], [O] or [N] table 2.1 illustrates the switching combinations for obtaining these states, where x represents the number of the leg (1, 2 or 3).

Table 2.1 Switching states for each phase in three-level T-type inverter.

Switching States	Status of switching devices (x=a,b,c) (1=ON , 0=OFF)				Output voltage
	S_{x1}	S_{x2}	S_{x3}	S_{x4}	V_{XO}
P	1	1	0	0	V_{dc1}
O	0	1	1	0	0
N	0	0	1	1	$-V_{dc2}$

• **[P]** State: In this state switches *Sx1* and *Sx2*, are ON, while *Sx3* and *Sx4*, are OFF. As a result, the phase voltage is $+V_{dc}/2$.

• **[O] state:** In this state, switches *Sx1* and *Sx4* are OFF while *Sx2* and *Sx3* are ON. Therefore, the phase output voltage in this state is clamped at zero.

• **[N] state:** In this state, switches *Sx1* and *Sx2* are turned OFF, while *Sx3* and *Sx4* are in ON-state. Hence, the output phase voltage is $-V_{dc}/2$ in this state.

It can be observed that the operations of switching devices in the same leg, such as a pair of *Sx1* and *Sx3* or a pair of *Sx2* and *Sx4*, are complementary. When one of them in a pair is switched ON, the other in the same pair must be OFF. The both-ON or both-OFF situation of the complementary devices is not allowed.

Moreover **t**he transition between [P] state and [N] state is prohibited. Therefore, the dynamic voltage sharing problem could be avoided in the three-level inverter. Furthermore, the magnitude of step changes of the output voltages in the three-level inverter is *V/2*, which is only half of that in traditional two-level inverters. As a result, less EMI is generated.

2.3.2.2 Inverter Switching States

Since the proposed T-type inverter has three per-phase switching states, there exist 27 switching states in the three-phase inverter, which are shown in Table 2.2.

The voltage vector can be grouped as follow:

I. Zero vector $\overrightarrow{V_0}$, representing three switching states [PPP], [OOO] and [NNN]. The magnitude of $\overrightarrow{V_0}$ is Zero.

II. Small vector ($\overrightarrow{V_1}$ to $\overrightarrow{V_6}$), all having a magnitude of $Vdc/3$. Each small sector has two switching states called (redundant switches).

III. Medium vectors ($\overrightarrow{V_7}$ to $\overrightarrow{V_{12}}$), whose magnitude is $Vdc * (\sqrt{3}/3)$.

IV. Large vectors ($\overrightarrow{V_{13}}$ to $\overrightarrow{V_{18}}$), all having a magnitude of $Vdc * (2/3)$.

Table 2.2 The 27 switching states of T-type inverter with their vector magnitude.

Space Vector	Switching State	Vector Classification	Vector Magnitude
$\overrightarrow{V0}$	[PPP],[OOO],[NNN]	Zero Vector	0
$\overrightarrow{V1}$	[ONN],[POO]	Small Vector	Vdc/3
$\overrightarrow{V2}$	[OON],[PPO]		
$\overrightarrow{V3}$	[NON],[OPO]		
$\overrightarrow{V4}$	[NOO],[OPP]		
$\overrightarrow{V5}$	[NNO],[OOP]		
$\overrightarrow{V6}$	[ONO],[POP]		
$\overrightarrow{V7}$	[PON]	Medium Vector	Vdc*($\frac{\sqrt{3}}{3}$)
$\overrightarrow{V8}$	[OPN]		
$\overrightarrow{V9}$	[NPO]		
$\overrightarrow{V10}$	[NOP]		
$\overrightarrow{V11}$	[ONP]		
$\overrightarrow{V12}$	[PNO]		
$\overrightarrow{V13}$	[PNN]	Large Vector	Vdc *($\frac{2}{3}$)
$\overrightarrow{V14}$	[PPN]		
$\overrightarrow{V15}$	[NPN]		
$\overrightarrow{V16}$	[NPP]		
$\overrightarrow{V17}$	[NNP]		
$\overrightarrow{V18}$	[PNP]		

Assuming the instantaneous voltage value of three-phase sine wave is respectively:

$$V_a = V_m * \sin(\omega t)$$
$$V_b = V_m * \sin(\omega t - 2\pi/3)$$
$$V_c = V_m * \sin(\omega t + 2\pi/3) \quad (2.1)$$

The magnitude and angle of the rotating vector can be found using Clark's Transformation where:

$$\overrightarrow{V_{ref}} = V_\alpha + jV_\beta = 2/3(V_a + aV_b + a^2 V_c) \quad (2.2)$$

Where: $a = e^{i2\pi/3}$

$$\left|\overrightarrow{V_{ref}}\right| = \sqrt{V_\alpha{}^2 + V_\beta{}^2}, \theta = \tan^{-1}(V_\beta / V_\alpha)$$

$$\begin{bmatrix} V_\alpha \\ V_\beta \end{bmatrix} = 2/3 \begin{bmatrix} 1 & -1/2 & -1/2 \\ 0 & \sqrt{3}/2 & -\sqrt{3}/2 \end{bmatrix} \begin{bmatrix} V_a \\ V_b \\ V_c \end{bmatrix} \quad (2.3)$$

2.3.2.3 Determining the sector

Now θ is calculated so we can know in which sector $\overrightarrow{V_{ref}}$ is located as follow:

- If θ is between 0° ≤ θ < 60°, then $\overrightarrow{V_{ref}}$ will be in Sector A.
- If θ is between 60° ≤ θ < 120°, then $\overrightarrow{V_{ref}}$ will be in Sector B.
- If θ is between 120° ≤ θ < 180°, then $\overrightarrow{V_{ref}}$ will be in Sector C.
- If θ is between 180° ≤ θ < 240°, then $\overrightarrow{V_{ref}}$ will be Sector D.
- If θ is between 240° ≤ θ < 300°, then $\overrightarrow{V_{ref}}$ will be Sector E.
- If θ is between 300° ≤ θ < 360°, then $\overrightarrow{V_{ref}}$ will be Sector F.

2.3.2.4 Determining the region in the sector

As already stated, wherever the reference voltage $\overrightarrow{V_{ref}}$ is located it can be represented using the three adjacent vectors in the region.

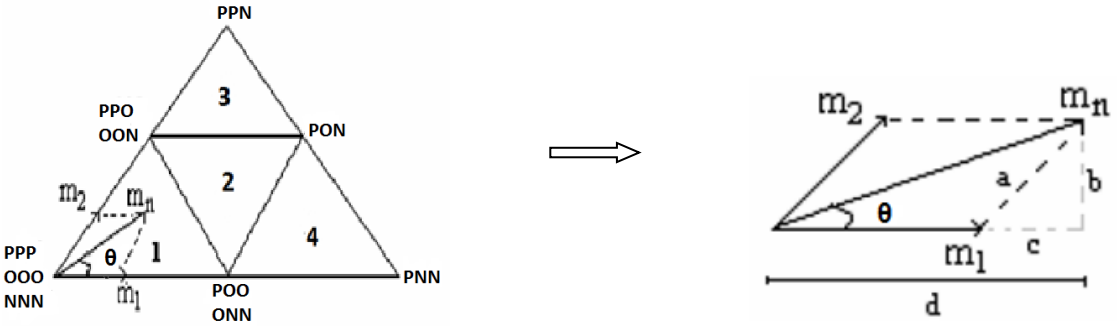

Figure 2.9 Space vector diagram for m1 and m2 in Sector A.

From Figure 2.9 m1 and m2 can be calculated as:

$$a = m_2 = \frac{b}{\sin(\frac{\pi}{3})} = \frac{2}{\sqrt{3}} b = \frac{2}{\sqrt{3}} m_n \sin\theta \quad (2.4)$$

$$m_1 = m_n \cos\theta - (\frac{2}{\sqrt{3}} m_n \sin\theta)\cos(\pi/3) = m_n(\cos\theta - \frac{\sin\theta}{\sqrt{3}}) \quad (2.5)$$

Then the sub-region can be detected as stated below:

- If m1, m2 and (m1 + m2) < 0.5, then $\overrightarrow{V_{ref}}$ is in Region 1.
- If m1 > 0.5, then $\overrightarrow{V_{ref}}$ is in Region 4.
- If m2 > 0.5, then $\overrightarrow{V_{ref}}$ is in Region 3.
- If m1 and m2 < 0.5 and (m1 + m2) > 0.5, then $\overrightarrow{V_{ref}}$ is in Region 2.

2.3.2.5 Dwell Times

By using sector A as an example, the calculation of the on time can be demonstrated below:

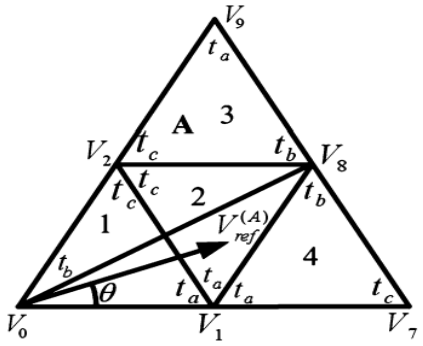

Figure 2.10 Vector combination in sector A.

Suppose $\overrightarrow{V_{ref}}$ laying in the region 2, so it can be composed by the three nearest vectors V1, V2 and V8 as illustrated in Figure 2.10. During a sampling period the equations for on time of the voltage vectors can be given as:

$$\begin{cases} \overrightarrow{V_{ref}}T_s = \overrightarrow{V_1} * t_a + \overrightarrow{V_8} * t_b + \overrightarrow{V_2} * t_c \\ T_s = t_a + t_b + t_c \end{cases} \tag{2.6}$$

$$\begin{cases} t_a = T_s - 2k\sin(\theta) \\ t_b = 2k\sin(\frac{\pi}{3} + \theta) - \mathrm{T_s} \\ t_c = \mathrm{T_s} - 2k\sin(\frac{\pi}{3} - \theta) \end{cases} \tag{2.7}$$

Where: $k = (\frac{4\sqrt{3}}{3})(\frac{V_{ref}}{E/2})\mathrm{T_s}$

Using the same procedure, the dwelling time in other regions in sector A can be obtained as shown in **Table 2.3**.

Table 2.3 ON Times in sector A.

On time / Region	t_a	t_b	t_c
1	$2K\sin(\frac{\pi}{3}-\theta)$	$Ts-2K\sin(\frac{\pi}{3}+\theta)$	$2K\sin(\theta)$
2	$Ts-2K\sin(\theta)$	$2K\sin(\frac{\pi}{3}+\theta)-Ts$	$Ts-2K\sin(\frac{\pi}{3}-\theta)$
3	$2K\sin(\theta)-Ts$	$2K\sin(\frac{\pi}{3}-\theta)$	$2Ts-2K\sin(\frac{\pi}{3}+\theta)$
4	$2Ts-2K\sin(\frac{\pi}{3}+\theta)$	$2K\sin(\theta)$	$2K\sin\left(\frac{\pi}{3}-\theta\right)-Ts$

2.3.2.6 Switching Sequence Arrangement

Generally, two design criteria have to be met during the switching sequence design in order to achieve the minimum device switching frequency.

1. The transition from one switching state to the next should involve only two switches, one being turned OFF and the other being turned ON; and
2. The transition from one triangular region to the next should involve minimum number of switching.

After calculating the ON time, the switching sequence has to be determined. As the converter has some redundant switching states, the switching sequence are arranged in order to achieve low THD and balancing the DC-link capacitors.

The switching sequences in the regions of sector (A) are arranged as follows:

Region 1: PPO-POO-OOO-OON-ONN and return.

Region 2: PPO-POO-PON-OON-ONN and return.

Region 3: PPO-PPN-PON-OON and return.

Region 4: POO-PON-PNN-ONN and return.

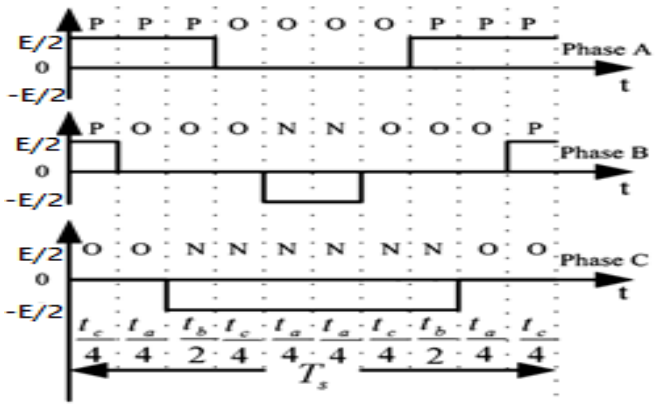

Figure 2.11 Switching sequence arranged in a symmetrical pattern.

According to switching sequences arranged in symmetrical pattern, the PWM firing time setting for each switch in sector A can be achieved as given in **Table 2.5**.

Table 2.4 PWM firing time setting for each switch of upper arms in sector (A).

Region / Time	1	2	3	4
PWM_S1a	$\frac{Tc}{4}+\frac{Ta}{4}$	$\frac{Tc}{4}+\frac{Ta}{4}+\frac{Tb}{2}$	$\frac{Ts}{2}-\frac{Tc}{4}$	$\frac{Ts}{2}-\frac{Ta}{4}$
PWM_S2a	$\frac{Ts}{2}$	$\frac{Ts}{2}$	$\frac{Ts}{2}$	$\frac{Ts}{2}$
PWM_S1b	$\frac{Tc}{4}$	$\frac{Tc}{4}$	$\frac{Tc}{4}+\frac{Ta}{2}$	0
PWM_S2b	$\frac{Ts}{2}-\frac{Ta}{4}$	$\frac{Ts}{2}-\frac{Ta}{4}$	$\frac{Ts}{2}$	$\frac{Ta}{4}+\frac{Tb}{2}$
PWM_S1c	0	0	0	0
PWM_S2c	$\frac{Ts}{2}-\frac{Ta}{4}-\frac{Tc}{4}$	$\frac{Tc}{4}+\frac{Ta}{4}$	$\frac{Tc}{4}$	$\frac{Ta}{4}$

2.3.2.7 Simplified Algorithm for SVM

The main idea of the simplified algorithm is how to achieve the Calculation Flow based only on one sector instead of six just by knowing the relationships in Dwell Time calculations and arrangement for switches between the first sector and the others as explained below.

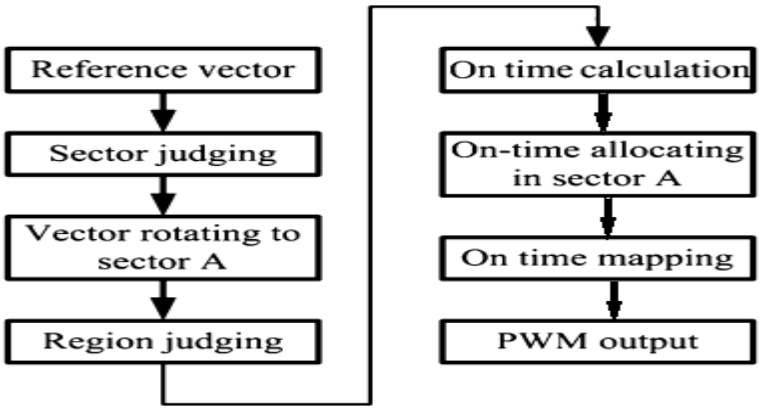

Figure 2.12 Simplified algorithm for SVM.

Suppose reference vector A stays in region 2 of sector A, while reference vector B is obtained by rotating vector A counterclockwise by 60° as shown in Figure 2.13. So the reference vector $V_{\text{ref B}}$ can be expressed in the following form:

$$V_{ref\_B}=V_{ref\_A}*e^{i\frac{\pi}{3}}=2/3(-V_b+(-V_c)e^{i\frac{2\pi}{3}}+(-V_a)e^{-i\frac{2\pi}{3}}) \quad (2.8)$$

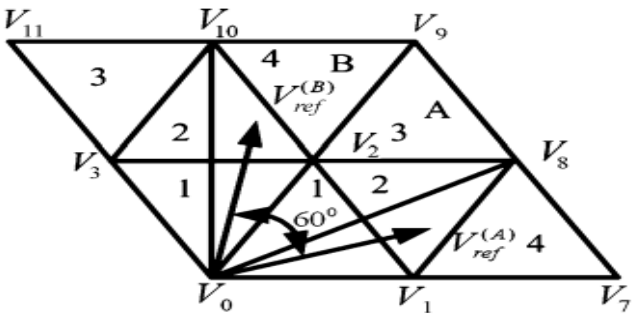

Figure 2.13 Two vectors with 60° shifting in the sector A and B.

When the reference vector is in the other sectors will be rotated to sector A by $n\pi/3$ where (n=1, 2, 3, 4, 5).

The corresponding reference vector in other sectors can be constructed as given in Table 2.5.

Table 2.5 Relationships of voltages constructing the reference vectors in six sectors.

Sectors	Phase Voltage A	Phase Voltage B	Phase Voltage C
A	U_a	U_b	U_c
B	$-U_b$	$-U_c$	$-U_a$
C	U_c	U_a	U_b
D	$-U_a$	$-U_b$	$-U_c$
E	U_b	U_c	U_a
F	$-U_c$	$-U_a$	$-U_b$

2.4 Conclusion

There are many types of power inverters, but only the T-type inverter provides the optimal solution between power quality and circuit complexity.

The principle of the space vector modulation for the three-level T-type inverter was introduced in this chapter. The power circuit and the switching states of the T-type inverter were described.

The space vector selection method was introduced and the dwell time calculation equations were derived. Based on the requirement of minimizing the device switching frequency, the switching state sequence of the inverter was developed.

Chapter Three

Design of Grid connected PV system

3.1 Introduction

Grid connected system without batteries are the simplest and cheapest solar power setup available, and the fact that it does not have to charge and maintain batteries they are also more efficient. Grid connected system can be decomposed into PV array, three-level inverter (T type), LCL filter and the grid utility. In order to achieve maximum power point tracking (MPPT), an adaptive golden section MPPT is used.

PV array is discussed in details in chapter one and the three level T-type inverter structure and controlling technique (SVM) details are presented in chapter two. This chapter will go in the details of the remaining parts of the grid connected PV system.

3.2 Grid Requirements for PV

As an important source of distributed generation (DS) the PV systems need to comply with a series of standard requirements in order to ensure the safety and the smooth transfer of the electrical energy to the grid.

There are lot of international standards that state constraints to inject power to the grid. The most relevant international regulations that are known worldwide are *IEC 61727* Characteristics, *VDE 0126-1-1* Standards (German regulations), *IEC 61000* Standards, *EN 50160* (in Europe) Standards and *IEEE 1547*, that latter has the longest history and probably is the most used standard [10].

In general, these standards deals with the following requirements:

- Voltage harmonic levels (THD).
- Voltage unbalance for three-phase inverter.
- Voltage amplitude and frequency variations.
- Voltage dips.

3.3 Voltage-Oriented Control

Grid connected system requires interfacing power electronic converters from the photovoltaic arrays to the grid. Such power electronic converters are mainly meant for two objectives. One is to ensure that the PV arrays are operated at the maximum power point (MPPT) and the other one is to inject a sinusoidal current into the grid.

Conventionally, these two functions are realized in two stages of power conversion, one is a DC/DC converter with MPPT control and the other one is a DC/AC power converter which is required to inject sinusoidal current to the grid at grid frequency.

A two-stage or sometimes called double-stage power conversion results in more power loss than that of a single-stage conversion.

A single stage grid-connected PV systems is proposed in this project where both the control objective i.e. extracting maximum power from the solar panel at different temperature and insolation level and injecting sinusoidal current into the grid at desired power factor are realized simultaneously in one power conversion stage. Such configuration will reduce losses and simplify the system topology [11].

The Block diagram of the whole system is given in Figure 3.1.and it consists of 2 main parts:

- the hardware part such as Solar panel string which represents the dc source, two symmetrical DC link capacitors, three-phase three-level inverter, LCL output filter, Line frequency transformer is employed to step up the inverter output voltage and inject it to the grid utility.
- Software part (The control part) consists of PLL (Phase-Locked Loop), MPPT algorithm, SVPWM, dc voltage control and PI current control loops.

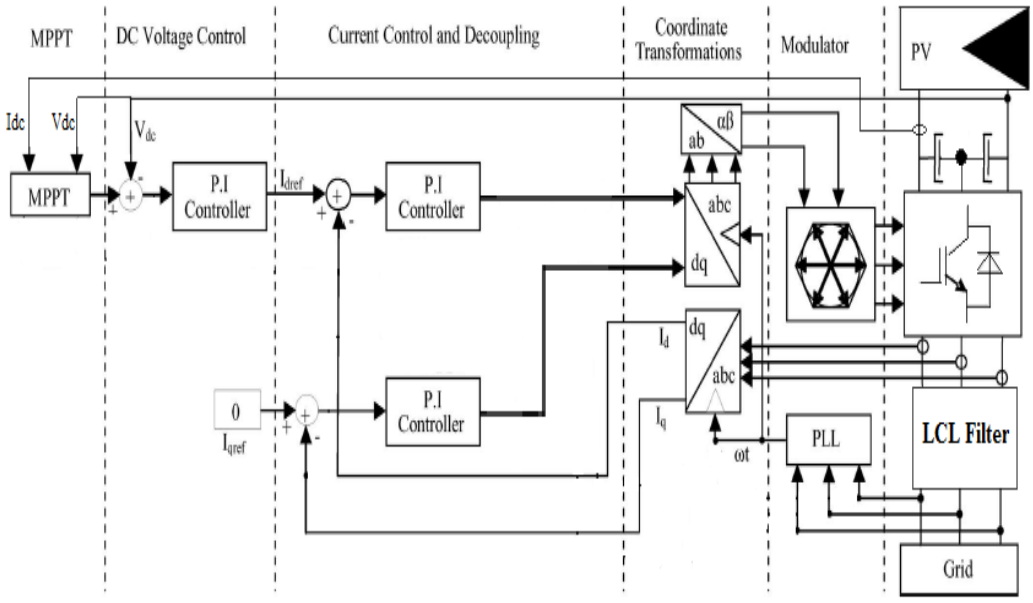

Figure 3.1 Grid-connected PV system with the proposed MPP tracker.

3.4 SVPWM mathematical model based on Three-Level Inverter

As stated in chapter two, the switching function for the three-level inverter is given by:

$$S_i = \begin{cases} 1 & \left(u_i = \frac{1}{2}\mathrm{E_d}\right) \\ 0 & \left(u_i = 0\right) \\ -1 & \left(u_i = -\frac{1}{2}E_d\right) \end{cases} \qquad (i = a, b, c) \tag{3.1}$$

In order to facilitate the analysis, we assume that all switches of the inverter are ideal.

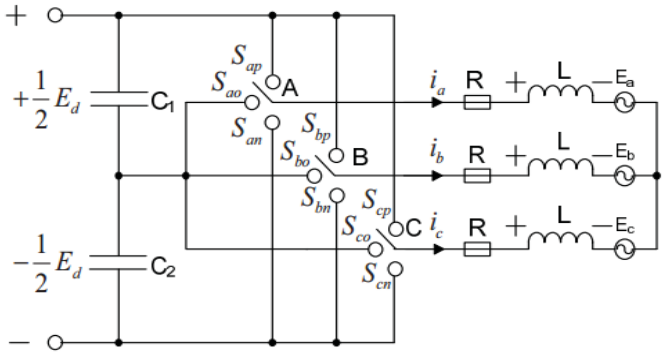

Figure 3.2 Simplified mode of three-level inverter [13].

As Figure 3.2 refers, a three-phase circuit's differential equations are driven as follow:

$$\begin{cases} U_{AN} = R i_a + L \dfrac{di_a}{dt} + E_a \\ U_{BN} = R i_b + L \dfrac{di_b}{dt} + E_b \\ U_{CN} = R i_c + L \dfrac{di_c}{dt} + E_c \end{cases} \tag{3.2}$$

Written as matrix form:

$$\begin{pmatrix} U_{AN} \\ U_{BN} \\ U_{CN} \end{pmatrix} = \begin{pmatrix} R & 0 & 0 \\ 0 & R & 0 \\ 0 & 0 & R \end{pmatrix} \begin{pmatrix} i_a \\ i_b \\ i_c \end{pmatrix} + \begin{pmatrix} L & 0 & 0 \\ 0 & L & 0 \\ 0 & 0 & L \end{pmatrix} \begin{pmatrix} \dfrac{di_a}{dt} \\ \dfrac{di_b}{dt} \\ \dfrac{di_c}{dt} \end{pmatrix} + \begin{pmatrix} E_a \\ E_b \\ E_c \end{pmatrix} \tag{3.3}$$

Furthermore, the relationship between load-phase voltage and inverter output voltage can be expressed as follows:

$$\begin{pmatrix} U_{AN} \\ U_{BN} \\ U_{CN} \end{pmatrix} = \frac{1}{6} E_d \begin{pmatrix} 2 & -1 & -1 \\ -1 & 2 & -1 \\ -1 & -1 & 2 \end{pmatrix} \begin{pmatrix} S_a \\ S_b \\ S_c \end{pmatrix} \tag{3.4}$$

Replacing equation (3.4) into (3.3) yields the main circuit mathematical model of the three-level inverter [13].

$$\begin{pmatrix} \frac{di_a}{dt} \\ \frac{di_b}{dt} \\ \frac{di_c}{dt} \end{pmatrix} = \begin{pmatrix} -\frac{R}{L} & 0 & 0 \\ 0 & -\frac{R}{L} & 0 \\ 0 & 0 & -\frac{R}{L} \end{pmatrix} \begin{pmatrix} i_a \\ i_b \\ i_c \end{pmatrix} + \begin{pmatrix} \frac{E_d}{6L} x\,(3S_a - S^*) - \frac{E_a}{L} \\ \frac{E_d}{6L} x\,(3S_b - S^*) - \frac{E_b}{L} \\ \frac{E_d}{6L} x\,(3S_c - S^*) - \frac{E_c}{L} \end{pmatrix} \tag{3.5}$$

Where: $S^* = S_a + S_b + S_c$

3.5 Maximum power point tracking (MPPT)

Due to the nonlinear voltage-versus-current characteristic of a photovoltaic (PV) array, there is a unique maximum power point (MPP) at which the PV operates to output maximum power. However, the MPP moves under different weather conditions because the output voltage and current of a PV array vary as the insolation and temperature change. The MPPT technique is necessary for a PV system to increase its energy generation efficiency, and thus to reduce its operating cost. In fact, a lot of MPPT methods have been proposed such as perturb and observe, incremental conductance method, and so on. It seems very difficult to determine which method among them is the best one. Nevertheless, this MPPT method using golden section search (GSS) algorithm is another competitive one because of its advantages of fast response, robust performance, and guaranteed convergence [14].

3.5.1 Perturb and observe (P&O) algorithm

Perturb and observe algorithm is also called hill climbing algorithm, as it is a standard MPPT algorithm it will be the first to be discussed in this section.

In this algorithm the MPPT method is based on the calculation of output power, such that any perturbation in the PV voltage leads to change in the output power of the system.

If the perturbation increases towards the maximum power point then voltage must be increased, on the other hand, if the perturbation decreases away from the maximum power point then the voltage must be decreased. With this V_{ref} that is the output of the algorithm is also continually changing and this process continues until the maximum power point is reached. Figure 3.3 clarify the flowchart of the P&O algorithm [17].

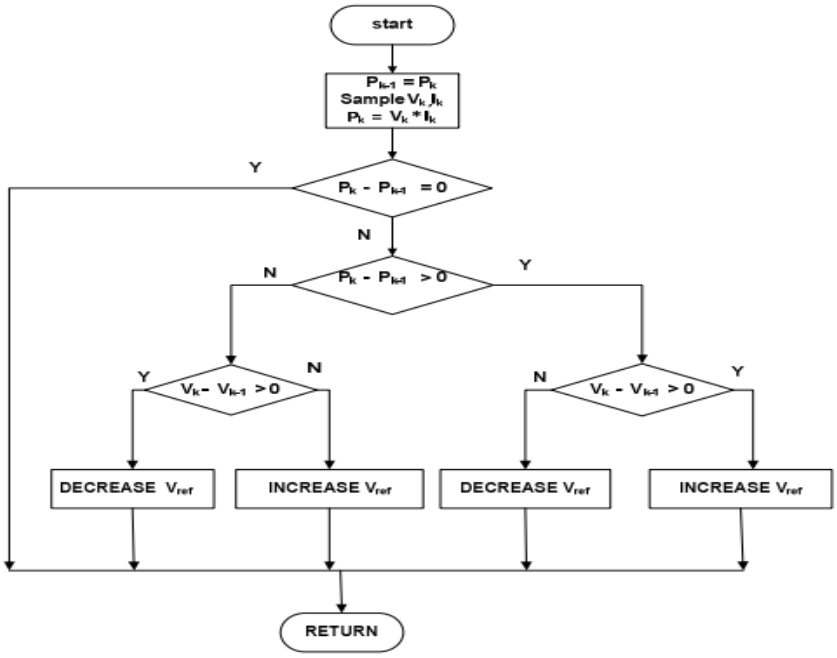

Figure 3.3 P&O MPPT flowchart [12].

3.5.2 Golden section search algorithm

The Golden Section Search (GSS) is a technique for finding the extremum (minimum or maximum) by sequential narrowing the range of values inside which the extremum exists. The main aim is to find maximum functional value of the function within an interval [a,b]. Two points x_1 and x_2 are selected in the interval [a,b] and the function is evaluated at these points, the points x_1 and x_2 are selected such that each point subdivides the interval into two parts satisfying the following relationship:

$$\frac{Length\ of\ the\ whole\ line}{Length\ of\ the\ larger\ fraction} = \frac{Length\ of\ the\ larger\ fraction}{Length\ of\ the\ smaller\ fraction} \tag{3.6}$$

Assume a line segment as shown in Figure 3.4 that is close to the P-V characteristics of the PV array, then as stated in equation 3.6:

$$\frac{1}{r} = \frac{r}{1-r} \Rightarrow r^2 + r - 1 = 0 \tag{3.7}$$

, hence, r =0.618

Knowing that:
$$\begin{cases} x_1 = b - r(b-a) \\ x_2 = a + r(b-a) \end{cases} \tag{3.8}$$

i.e. x_1 is 0.618 of interval away from ‘b‘ and x_2 is 0.618 of interval away from ‘a‘.

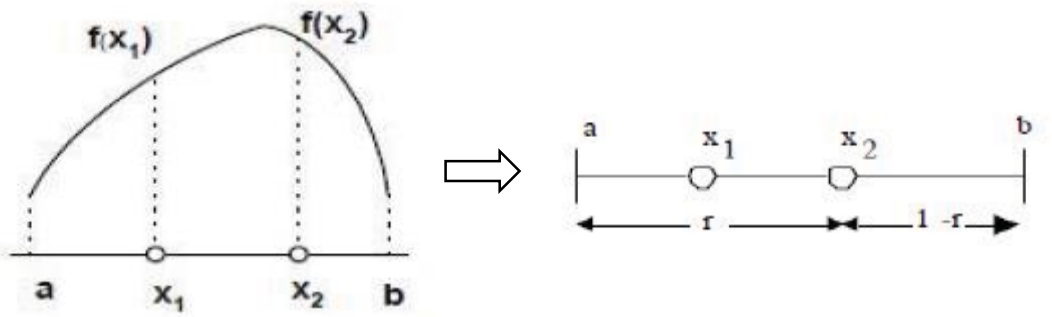

Figure 3.4 Interval markings of a function f(x) [14].

When GSS is applied to photovoltaic system for maximum power point tracking, the voltage is used as the search variable; the GSS computes the voltage (V_{ref}) that corresponds to the maximum power point for the corresponding operating conditions i.e. irradiation and temperature level.

The P-V characteristics correspond to power whose maximum value has to be tracked and is represented by f(x), whereas x_1 and x_2 correspond to the array voltage. The range of operation is from zero to open circuit voltage (V_{oc}), i.e. a=0 and b=V_{oc}. The flowchart for finding the maxima of a function using GSS is shown in Figure 3.5 [14].

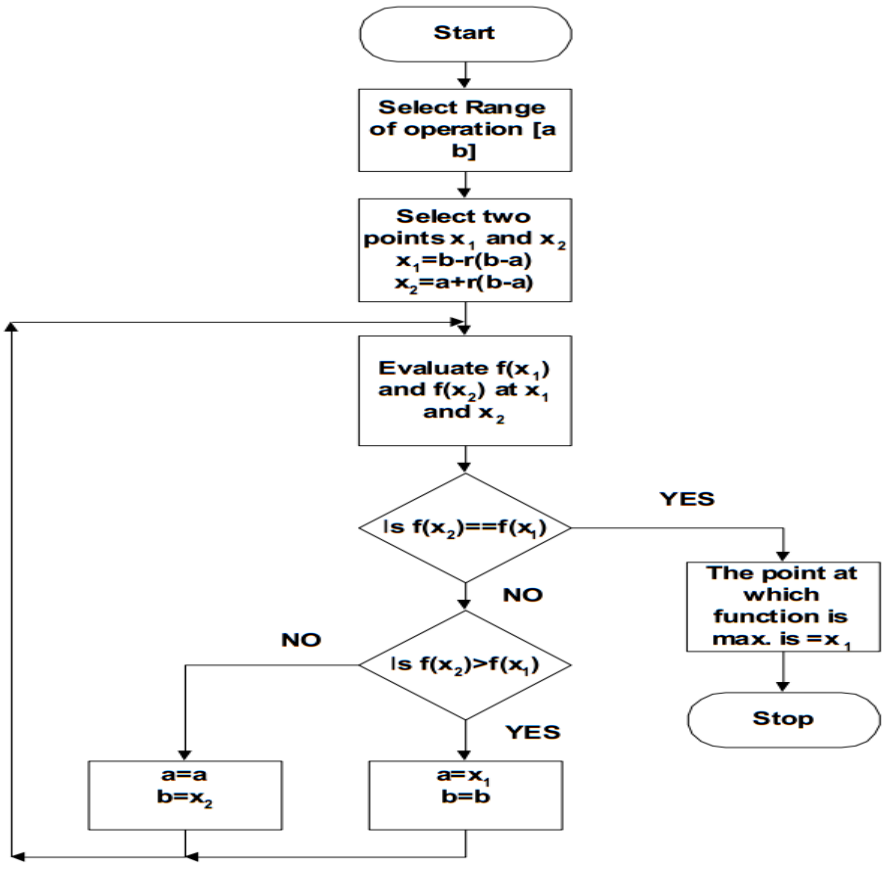

Figure 3.5 Flowchart of GSS algorithm [14].

3.6 Closed loop inverter control

The grid voltages and line currents are transformed into d-q reference frame (park transformation) at the angular frequency of the utility grid ω that is extracted from the PLL to be used as feedback variables for the controller.

3.6.1 Park Transformation

The three phase AC voltage (current) quantities are converted into rotating reference frame quantities (DC quantities) and vice versa using Park transformation as follow [18]:

$$\begin{pmatrix} V_d \\ V_q \\ V_0 \end{pmatrix} = T_{dq0}(\theta) \begin{pmatrix} V_a \\ V_b \\ V_c \end{pmatrix} \Leftrightarrow \begin{pmatrix} V_a \\ V_b \\ V_c \end{pmatrix} = \left[T_{dq0}(\theta) \right]^{-1} \begin{pmatrix} V_d \\ V_q \\ V_0 \end{pmatrix} \tag{3.9}$$

Where:

$$T_{dq0}(\theta) = \frac{2}{3} \begin{bmatrix} \cos(\theta) & \cos(\theta - \frac{2\pi}{3}) & \cos(\theta + \frac{2\pi}{3}) \\ \sin(\theta) & \sin(\theta - \frac{2\pi}{3}) & \sin(\theta + \frac{2\pi}{3}) \\ \frac{1}{2} & \frac{1}{2} & \frac{1}{2} \end{bmatrix} \tag{3.10}$$

θ is the angular displacement of Park's reference frame.

These transformations are implemented in MATLAB/ Simulink to convert the three phase AC quantities into DC quantities so that control scheme can be implemented.

3.6.2 Phase-Locked Loop (PLL)

A grid-connected power converter perfectly matches the PLL's theory since it should work in harmony with the grid. It should phase-lock its internal oscillator to some particular grid power signal in order to generate an amplitude and phase-coherent internal signal that is used by different blocks of the control system. The output signal (ωt) of PLL block is a ramp that varying between 0 and 2*pi and take the frequency of the grid (50Hz) as shown in figure 3.6 below [19]:

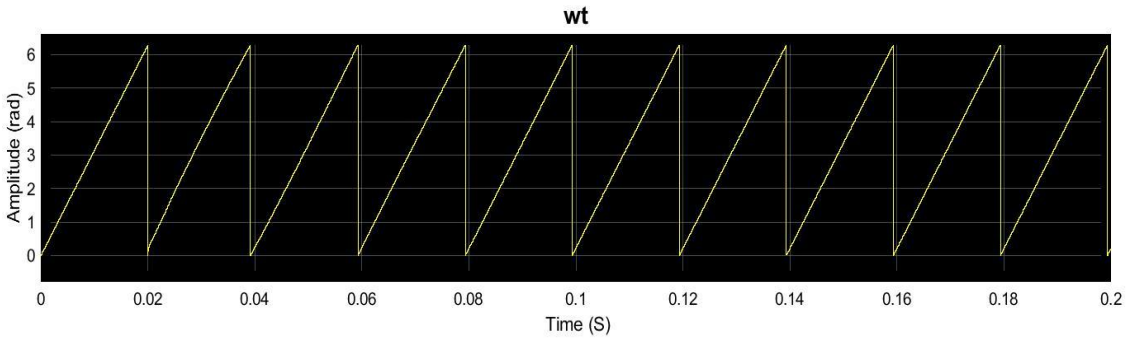

Figure 3.6 PLL output signal (ωt).

3.6.3 Voltage oriented control strategy

The voltage oriented control was based on the synchronously rotating d-q axis frame. The VOC had two control loops, the inner current loop, and the voltage outer loop. According to the mathematical model of the three-level inverter discussed in section 3.3:

$$\begin{cases} L\dfrac{di_d}{dt} = -Ri_d + \omega L i_q - V_d + e_d \\ L\dfrac{di_q}{dt} = -Ri_q + \omega L i_d - V_q + e_q \end{cases} \tag{3.11}$$

3.6.3.1 Inner current loop control

Equations (3.11) show that i_d and i_q are coupled, which means that when one is being controlled, then the other one will be altered. So, the decoupling control needs to be carried on in order to control them independently. The strategy of feed forward decoupling control is used, making:

$$Ri_d + L\frac{di_d}{dt} = (K_p + \frac{K_I}{S})(i^*_d - i_d) \tag{3.12}$$

$$Ri_q + L\frac{di_q}{dt} = (K_p + \frac{K_I}{S})(i^*_q - i_q) \tag{3.13}$$

Replacing equations (3.11), (3.12) in equation (3.13) we get:

$$V_d = -(K_p + \frac{k_I}{S})(i^*_d - i_d) + \omega L i_d + e_d \tag{3.14}$$

$$V_q = -(\mathrm{K_p} + \frac{K_I}{S})(i^*_q - i_q) + \omega L i_q + e_q \tag{3.15}$$

According to the equations (3.14) and (3.15), i_d and i_q can be controlled independently after decoupling. Then, the active and reactive powers, respectively, can be controlled independently, and this can make the design of the current loop much easier. The principle current loop controller is presented in Figure 3.1 above.

3.6.3.2 Outer DC voltage control loop

The main function of the outer voltage loop control is to regulate the DC link voltage and to generate the reference current i_d for the current inner loop. To design the voltage outer loop to ensure the unity power factor, the reactive power component (i_q) should be equal to zero. The outer voltage control based on the PI controller connecting with inner current loop control is shown in Figure 3.1 above [20].

3.7 Active and reactive power control

In the synchronous rotating frame d-q, the active and reactive powers of a three-phase grid-connected VSI are given by:

$$\begin{cases} P = \frac{3}{2}(V_d i_d + V_q i_q) \\ Q = \frac{3}{2}(V_d i_q - V_q i_d) \end{cases} \quad (3.16)$$

If the three-phase grid voltage is ideally sinusoidal without any harmonics, then in the dq frame, the grid voltage vector is given by:

$$\begin{cases} V_d = V \\ V_q = 0 \end{cases} \quad (3.17)$$

In practice, the grid voltage is non-sinusoidal due to harmonics. Therefore, both V_d and V_q will not be constant but have slight ripples whose frequencies and magnitudes depend on the harmonic components. However, in steady state, the average value of V_q is still equal to zero. Consequently, (3.16) can be rewritten as (3.18). Hence, its active power depends on the d-axis current, and the reactive power depends on the q-axis current. Furthermore, in order to achieve unity power factor fundamental current flow, the q component of the command current vector is set to zero.

$$\begin{cases} P = P_{pv} = \frac{3}{2}(V_d i_d) \\ Q = \frac{3}{2}(V_d i_q) \end{cases} \quad (3.18)$$

Equation 3.18 allows one to obtain the relation:

$$i_d = \frac{2}{3V_d} P_{pv} \quad (3.19)$$

Therefore, the PV power information can be obtained from the d-axis grid current component by the relation (3.19) [12].

3.8 LCL filter parameters design

Compared with the L filter or LC filter, the LCL filter can use a smaller inductance to achieve the same filtering effect, which has great importance in reducing the cost and size of filter. The LCL filter is a third-order system and the existence of resonance problems can be suppressed by increasing damping coefficient in the system.

3.8.1 Mathematical model of LCL filter

The single-phase equivalent diagram of the LCL filter is shown in Figure 3.7 u_{inv} is the output voltage of the T-type three-level inverter, and (i_1) is the current through arm side inductance (L_1) and resistance (R_1). Current (i_2) flows through the grids-side inductance (L_2), resistance (R_2) and the power grid e. Current i_c flows to the filter capacitor whose voltage is u_c.

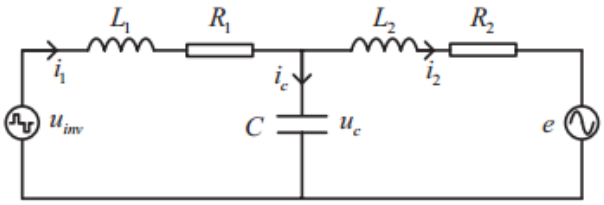

Figure 3.7 The single-phase equivalent diagram of the LCL filter [7].

Ignore parasitic resistance of the filter inductor, then R_1=R_2=0. The equivalent circuit of the LCL filter can be obtained as Figure 3.8.

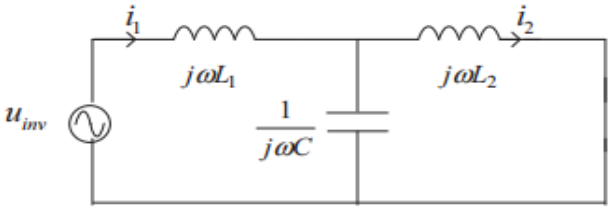

Figure 3.8 The simplified equivalent diagram of the LCL filter [7].

The reactive power of the LCL filter generated by the filter capacitor must be less than 5% of the rated power in the inverter, thereby the value range of filter capacitance can be determined as below.

$$C < \frac{5\%\,\mathrm{P}}{6\pi\,\mathrm{f}\,e^2} \tag{3.20}$$

Where P is the PV array's power, (e) and (f) are the grid phase voltage and frequency respectively.

The voltage of the filter inductor in the LCL filter must be less than 10% of that in the grid-side, which can determine the upper limit of the total value of inductance according to.

$$L_1 + L_2 < \frac{10\% e^2}{2\pi \text{fP}} \tag{3.21}$$

In order to minimize noise and loss of the inverter, $L1$ should be 3 to 5 times larger than $L2$ depending on the resonance frequency.

The resonance frequency f_{res} should be taken in between 10 times and an half time of the switching frequency f_s in order not to make the resonance frequency occur at the high frequency nearby the switching frequency or low frequency nearby the fundamental frequency. Since the LCL filter has resonance problems, the value rang of f_{res} is showed in (3.22).

$$10f \leq f_{res} \leq \frac{f_s}{2} \tag{3.22}$$

3.9 Total harmonic distortion

The total harmonic distortion, or THD of a signal is a measurement of the harmonic distortion present in the signal and is defined as the ratio of the sum of the powers of all harmonic components to the power of the fundamental frequency. Hence, Current THD is the ratio of the root-sum-square (RMS) value of the harmonic contents of the signal to the (RMS) value of the fundamental current. According to IEEE standards the current THD must be less than < 5% to inject power to the grid [7].

$$THD_{avg}[\%] = \int_0^T \left[\frac{\sqrt{\sum_{h>1} I_h^2}}{I_1} \times 100 \right] dt \tag{3.32}$$

3.10 Conclusion

To maximize the power delivered by the PV array and improve the efficiency MPPT algorithms are unavoidable, one of the most efficient MPPT algorithms is the Golden section search (GSS).

However in order to inject this power to the grid utility, strict standards must be satisfied, for that complicated control loops must be implemented in addition to well-tuned filtering device have to be integrated to the system.

Chapter Four

Simulation and Implementation

4.1 Introduction

The next step after going through the theoretical part of the single stage grid connected PV system is to enhance it with practical results. To do so a simulation of the system is essential to assure the safe and correct working of each part of the system before passing to the implementation where any error is prohibited.

This section presents the model and simulation results of PV system single stage three-phase three-level T-type grid interactive inverter.

4.2 Simulation part

4.2.1 Single stage grid connected PV system Simulink model

Computer simulation has been done using MATLAB/SIMULINK simulation package. The full simulation mode of the system is shown in Figure 4.1.

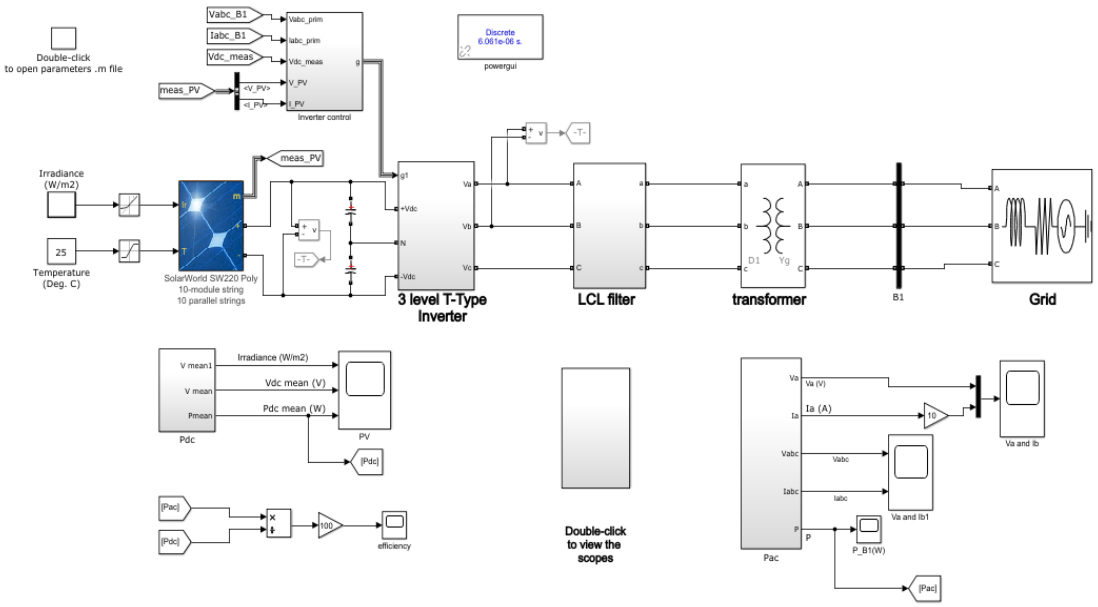

Figure 4.1 The whole system Simulink model.

The PV array is chosen to be a SolarWorld SW220 Poly one with 10 parallel strings each one contains 10 series connected modules, providing the P-V characteristics presented in figure 4.2.

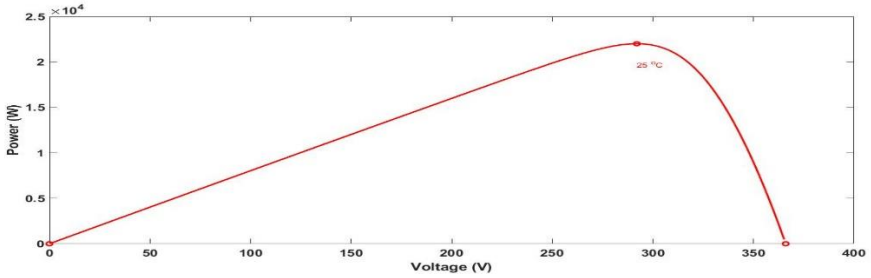

Figure 4.2 The P-V characteristics of the PV array used in the simulation.

Two identical DC link capacitors with values of 0.0155F are directly coupled to the PV array to split the DC voltage and create the neutral point for the three level inverter.

4.2.1.1 The three level T-type inverter Simulink model

The three phase three level T-type inverter used in the system and its controlling that is the SVM are presented in figures 4.3 and 4.4 respectively, the switching frequency is set to 10KHz. The line and phase output voltages of the inverter are shown in figure 4.5.

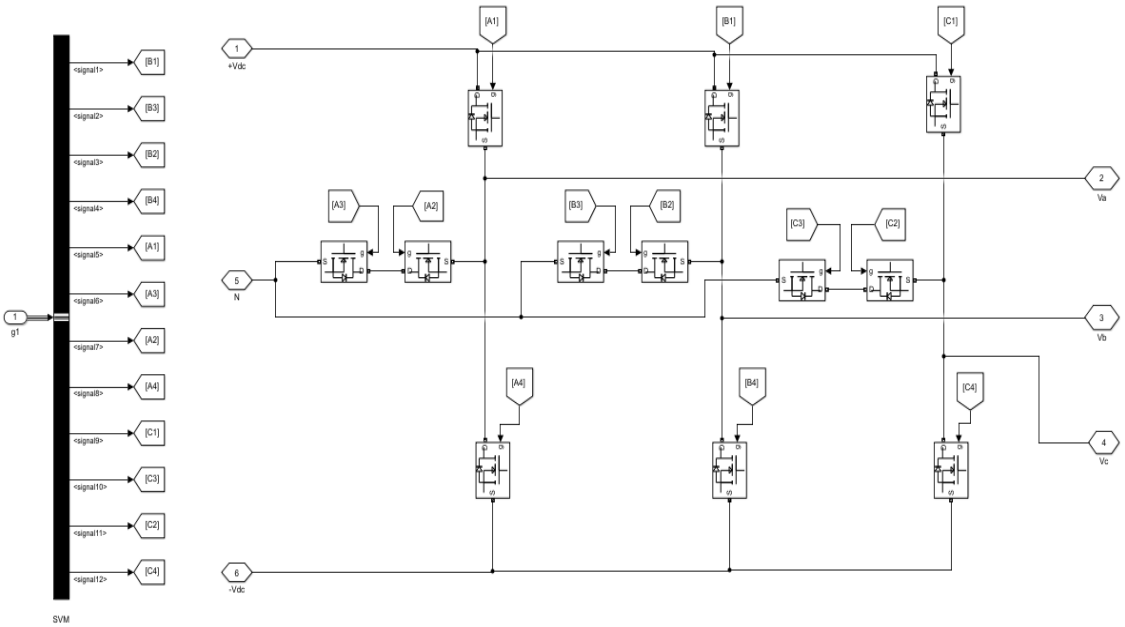

Figure 4.3 The Simulink model of the T-type inverter used.

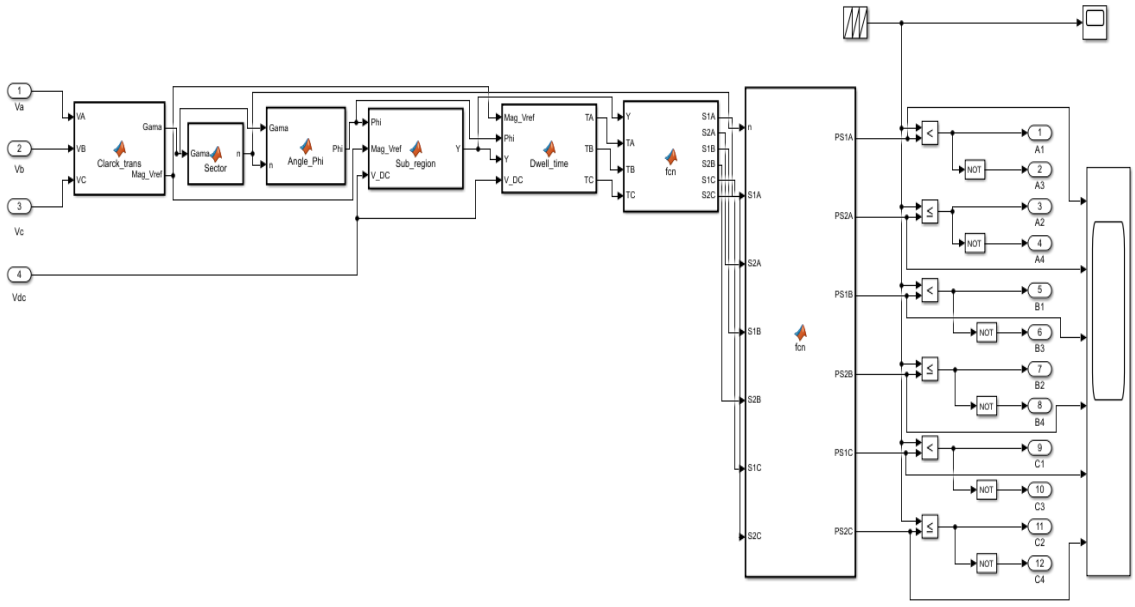

Figure 4.4 The SVM technique Simulink model.

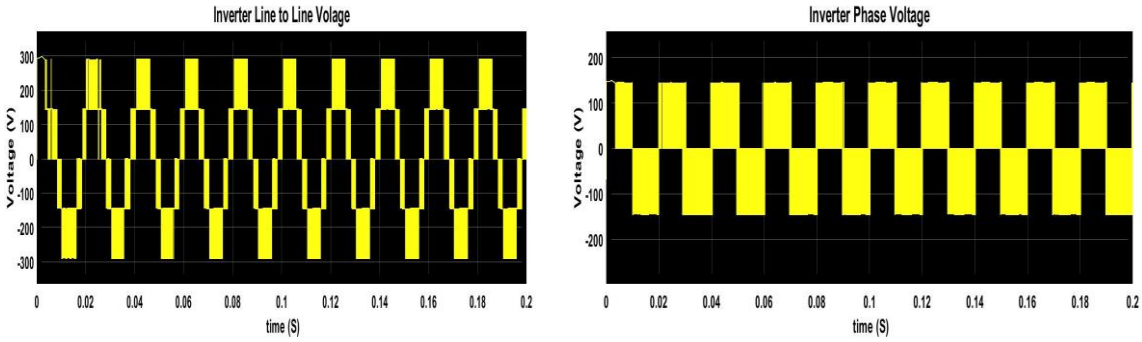

(a) **(b)**

Figure 4.5 Inverter output voltage: **(a)** Line voltage and **(b)** Phase voltage.

Discussion:

The output voltage of the inverter is as expected, the line voltage consists of three steps (levels); zero, Vdc/2 and Vdc. Hence, the name three level inverter is deriver. The small distortion at the beginning is due to the fact that the PV voltage takes time to build up, this causes an over modulation.

4.2.1.2 The LCL filter Simulink model

The filtering device is shown in figure 4.6 where all high frequency harmonics are eliminated to give a smooth sinusoidal current at the output as shown in figure 4.7.

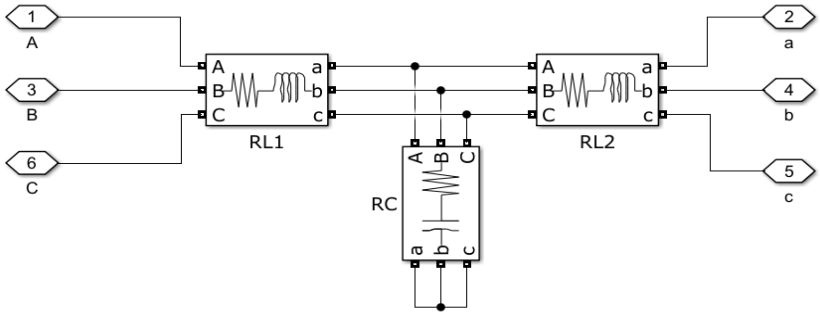

Figure 4.6 The LCL filter Simulink model.

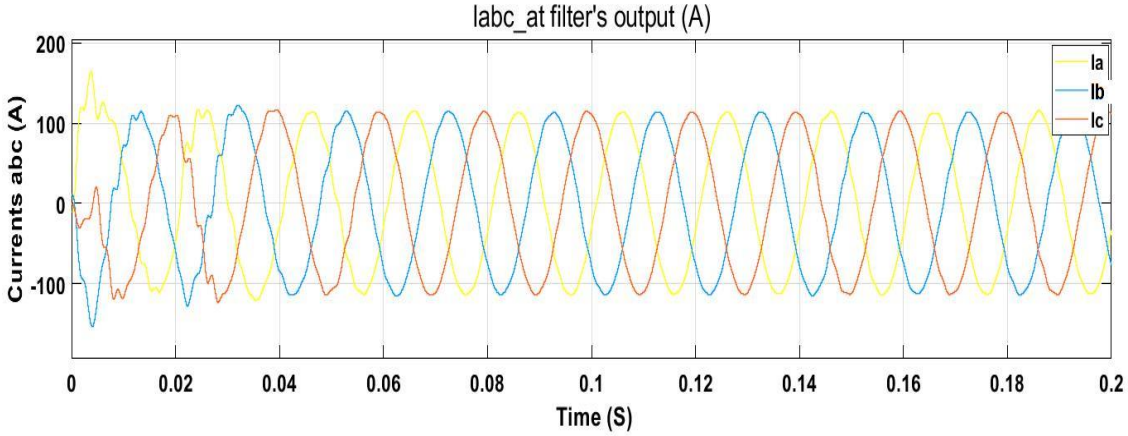

Figure 4.7 The three phase currents at the LCL filter output.

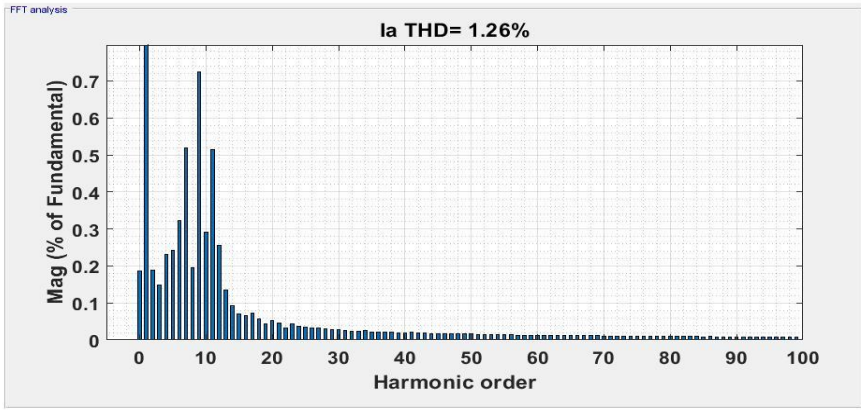

Figure 4.8 The FFT analysis of the filter output current.

The filter parameters are set to be as follow (refer to section 3.8 for more details):

$$\begin{cases} R_1 = R_2 = 0.00157388\Omega \\ L_1 = L_2 = 5.0098e\text{-}04H \\ R = 0.2098\Omega \\ C = 3.03489e\text{-}04F \end{cases}$$

Discussion:

As it is shown in figure 4.8, the THD of the filter output current is 1.53% that is within the IEEE standards for grid power injection, which means that the LCL filter is well tuned to perform the filtering role.

4.2.1.3 Maximum power point tracking 'MPPT'

Two MPPT algorithms were implemented in this simulation, the classical Perturb and Observe algorithm and the powerful Golden Section Search. However to complete the single stage tracking of the maximum power, these algorithms collaborate with two controlling loop, the current loop (figure 4.10) and the voltage loop(figure 4.11).

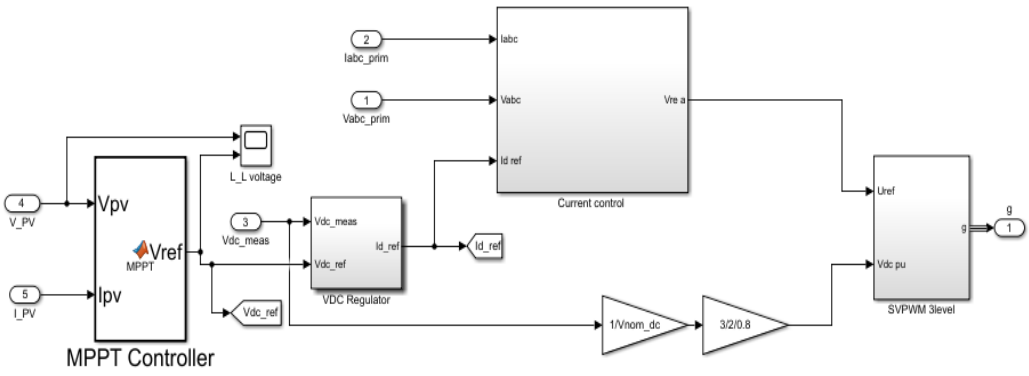

Figure 4.9 The MPPT Simulink model.

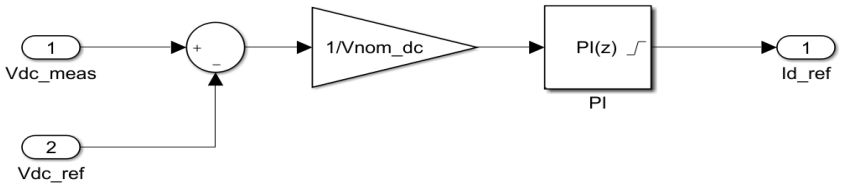

Figure 4.10 Vdc regulator model.

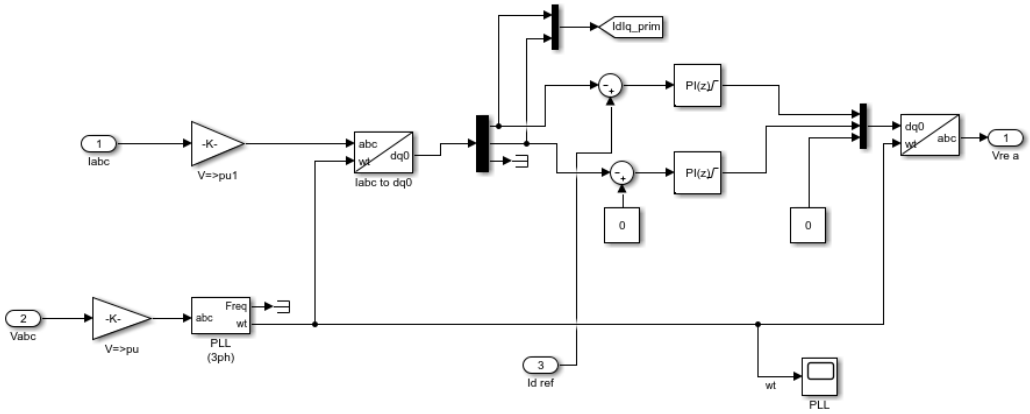

Figure 4.11 Current controller Simulink model.

The PIs parameters of both controllers were tune using manually and the best results were gotten for the following values:

$$\begin{cases} K_{p\_v} = 50 \\ K_{I\_v} = 9000 \end{cases} \quad \text{and} \quad \begin{cases} K_{p\_I} = 1 \\ K_{I\_I} = 100 \end{cases}$$

Iq is set to zero to make the system operating at unity PF, figure 4.12 shows the phase shift between Va and Ia (Ia is multiplied by 10 to make the phase shift clearer).

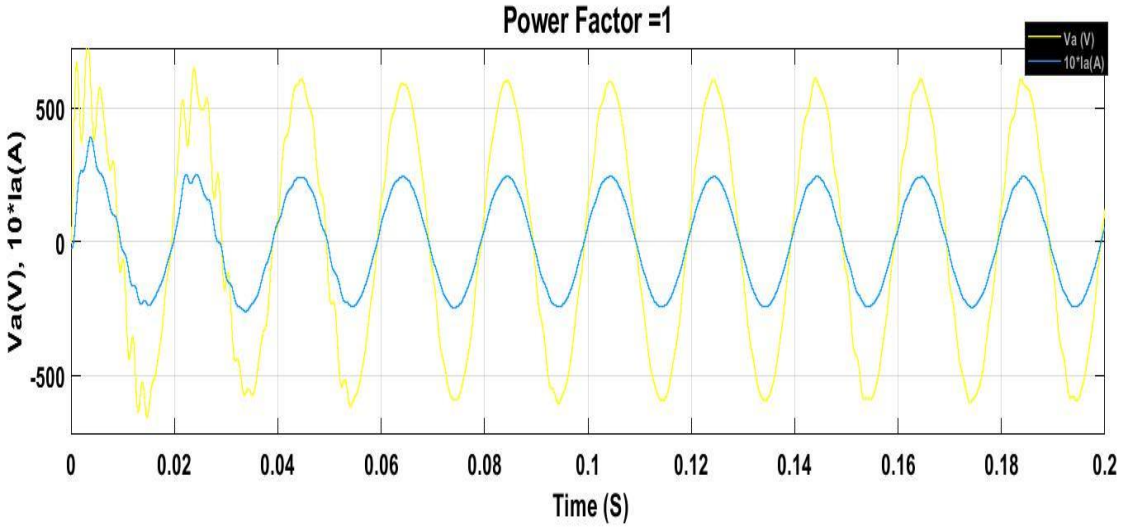

Figure 4.12 The phase shift between Va and Ia.

A typical three-phase 2.2KW 150/707V transformer is used to step up the voltage and provide an isolation function between the PV system and the high power grid.

Over the simulation time, the temperature is kept constant at 25°C while the irradiance is changed from 1000W/m² to 500W/m² then back to 1000W/m². Figures 4.13 and 4.14 shows how the PV voltage follow the MPPT reference voltage. While figures 4.15 and 4.16 shows the PV power that is delivered by the PV array using both GSS and P&O algorithms.

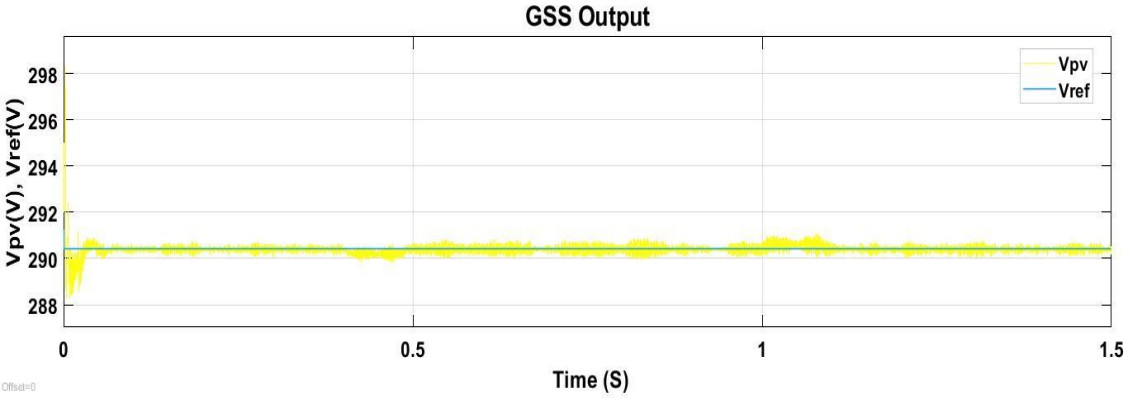

Figure 4.13 The GSS output (Vref) compared with PV voltage (V_PV).

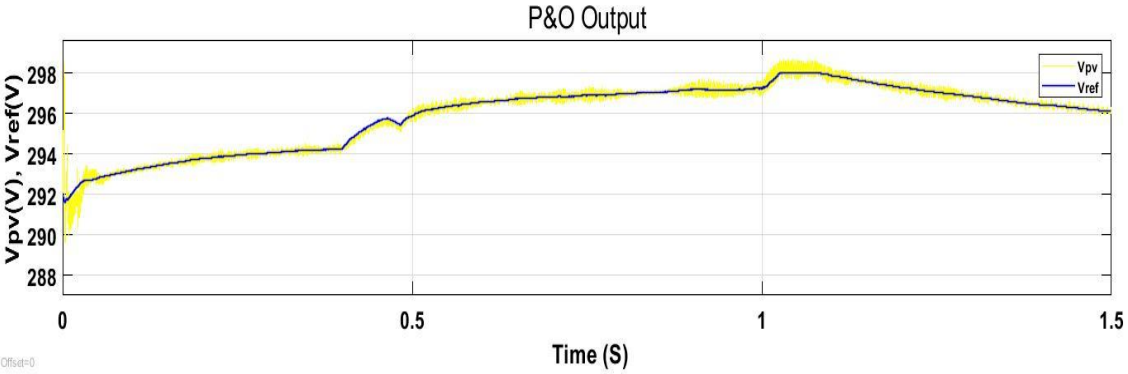

Figure 4.14 The P&O output (Vref) compared with PV voltage (V_PV).

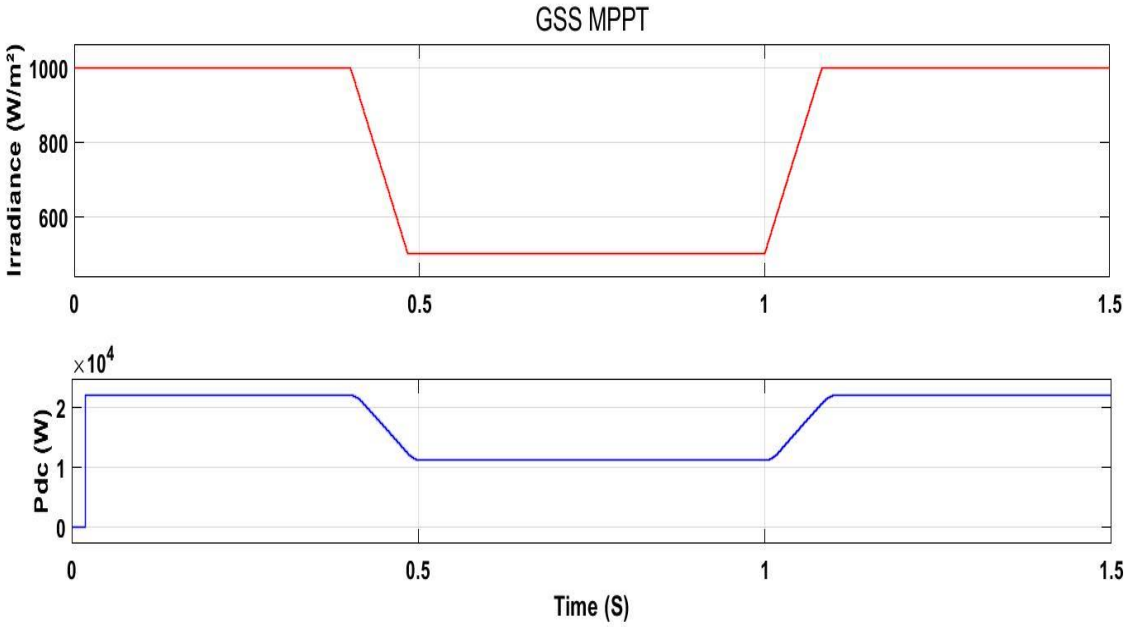

Figure 4.15 The delivered PV power for variable irradiance using GSS.

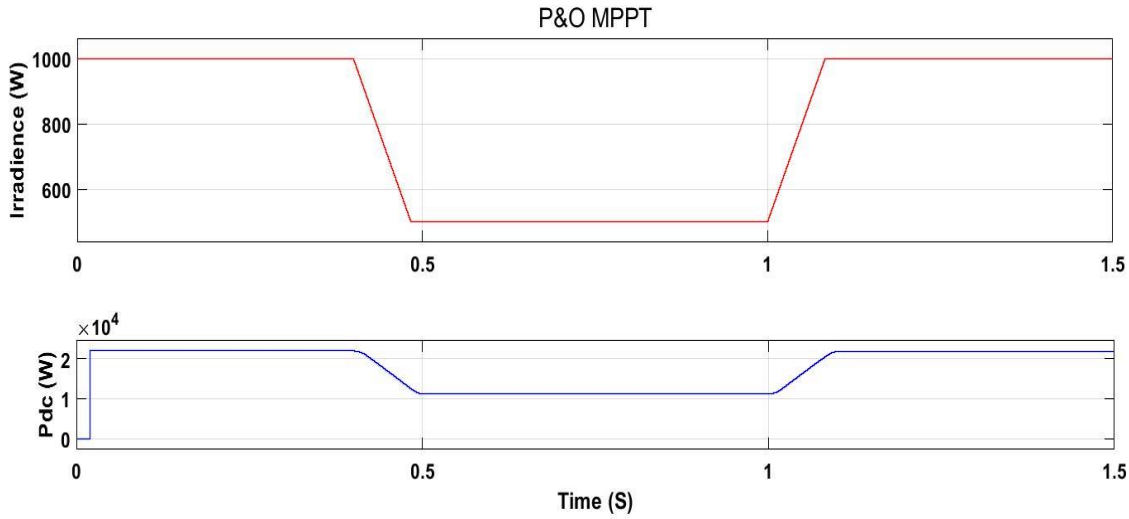

Figure 4.16 The delivered PV power for variable irradiance using P&O.

Zooming enough the deference between the GSS response and that one of P&O will appear as shown on figure 4.17.

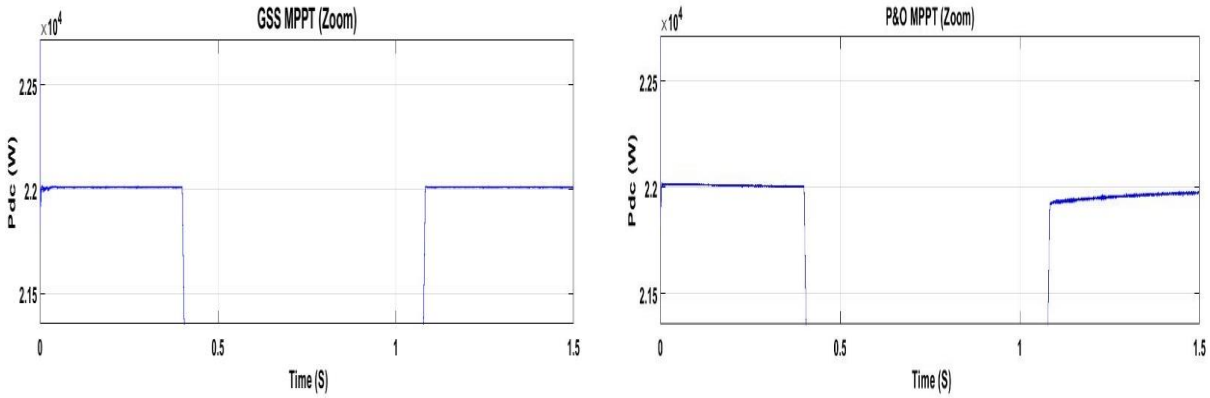

(a) **(b)**

Figure 4.17 Zoom of the responses (a) Zoom of figure 4.15, (b) Zoom of figure 4.16.

The three phase voltages and currents at the grid bus under variable irradiance using either MPPT algorithms lead to roughly the same response as shown in figure 4.18.

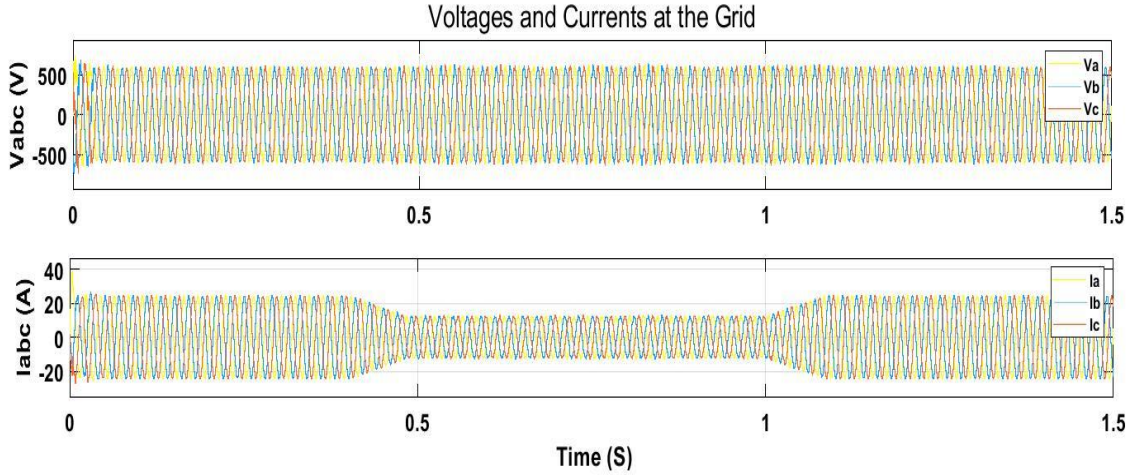

Figure 4.18 Three phase currents and voltages at the grid bus under variable irradiance.

Finally, the system efficiency that is the input (PV) power over the output (Grid) power (figure 4.19) using either MPPT algorithms lead to approximately the same efficiency as shown in figure 4.20.

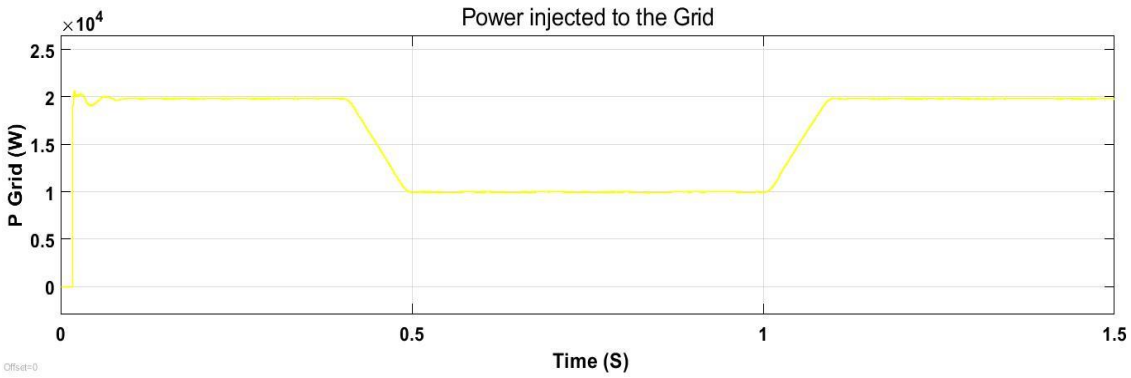

Figure 4.19 The power at the grid bus.

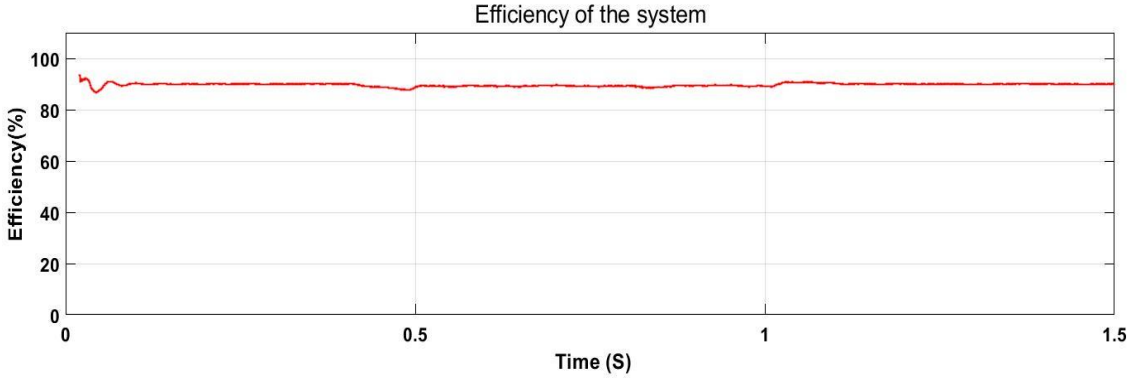

Figure 4.20 The system efficiency.

Discussion:

As it is clearly mentioned in figures 4.14 and 4.15 the MPPT algorithms used in the simulation are effectively tracking the maximum power point regardless of the irradiance. Setting Iq to zero makes the system operates at unity PF, which means that the system exports only active (useful) power to the grid.

The advantage of the GSS over the classical P&O algorithm is the fast convergence to the MPP (figure 4.12) and its ability to track the MPP even ender shading effect.

The total system efficiency is around 90%; in fact, this is due to the system losses at each level starting from the switching losses of the inverter to the losses in the damping resistances used in the LCL filter and coming to the power transformer losses.

4.3 Implementation Part

Generally, the implementation of three-level three phase T-type inverter consist of three main stages. The first stage is programing the STM32F4 discovery board by writing the algorithm code in MATLAB Function that is able to generate the desired

pulses, then designing and implementing the gates driving circuitry, then ending up by the power circuitry that will be responsible for generating the three-phase three level voltage signal. The logic is depicted in the figure below:

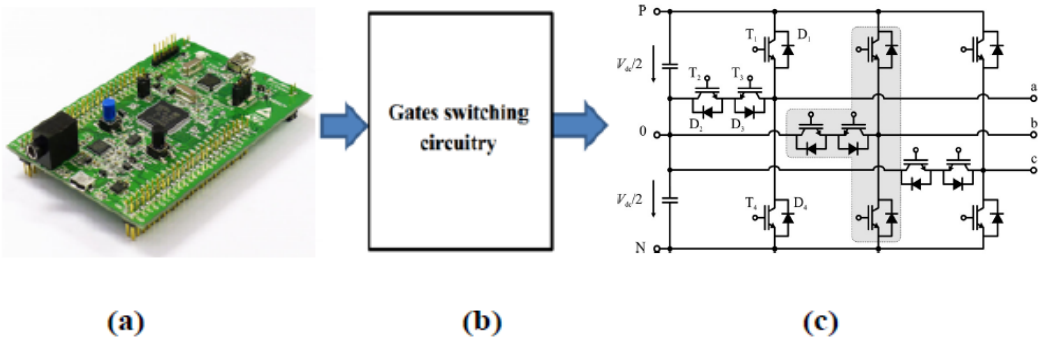

Figure 4.21 (a) STM32F4 Discovery board, **(b)** Gates driving circuit, **(c)** T-type inverter Power circuit.

4.3.1 Introduction to STM32F4 DISCOVERY board

The ST Microelectronics STM32F407 arm cortex micro controller is world's highest performance cortex M series micro controller. The main specification of STM32F4.

Discovery kit:

-Discovery board fitted with STM32F4 microcontroller running at 168MHz.

-Power supply with transformer and mains cable.

-Evaluation version of the keil MDK-ARM development kit which includes a cross complier, assembler and debugger.

STM32F407 micro controller in an LQFP100 package running at 168MHz (max) providing peak through out of 210 MIPs; hardware level debugging is done by on board ST-LINK/V2 debugger (SWD connector for programming and debugging).There are various on chip peripherals are available such as ADC, DAC, GPIOs, Timers and USART [21].

4.3.2 Pulse (SVM) generation using STM32F4 board

Experimental results were obtained by applying the proposed SVM method using STM320F4. The source code was written in MATLAB Function blocks (**Figure 4.22**) then compiled and uploaded to the board to get the desired switching patterns at the output pins, the switching frequency is selected to be 5 kHz.

To run model file user needs two hardware:

• ST Microelectronics STM32F4 discovery board.

• USB type A to mini B cable.

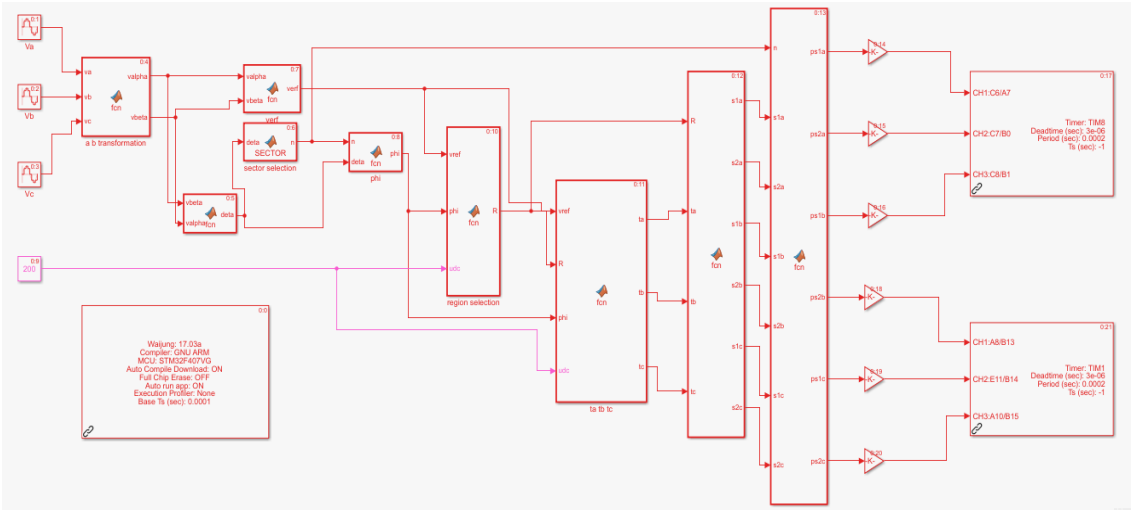

Figure 4.22 Embedded simulated model for Three Phase SVM Technique in STM32F4 Discovery Kit in Waijung Simulink library.

The switching signals at the output pins of the STM32F4 board and their fundamental signals gotten using RC filter, as shown in figure 4.23.

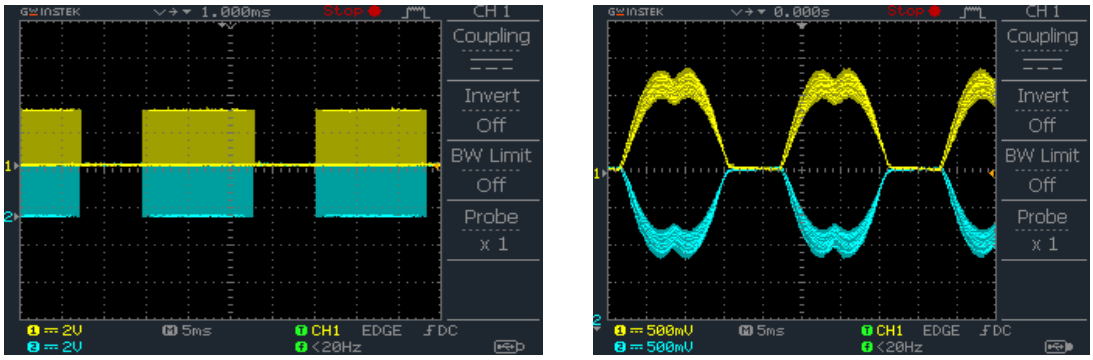

(a) **(b)**

Figure 4.23 (a) The gate signal and its inverse generated by STM32F4. **(b)** The fundamental signals.

The dead time necessary to avoid the short circuit case was introduced in the switching signals using the embedded STM model and is chosen to be 3µs as it is clear in figure 4.24.

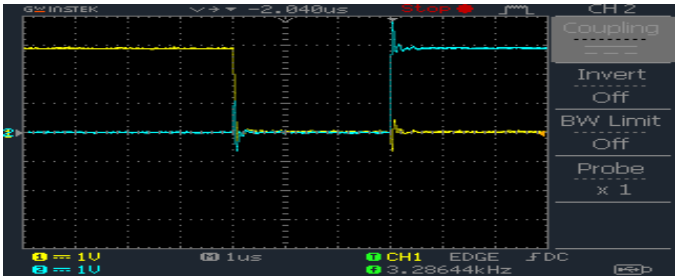

Figure 4.24 The dead time between two switches Sa1 and Sa3.

4.3.3 Power supply circuit

Buffers and optocouplers all need DC power supply. In general, for solar systems, DC power supplies are provided using batteries or directly from the panels. However, in this study, components are fed using the grid's power.

A step down transformer that converts the 110 V AC to 15 V AC, a Wheaston bridge for signal rectification, 470 μF/50V smoothing capacitor to remove the ripples, and 15V zener diode and 1kΩ resistor to generate the desired voltages +15V and -5V that feeds the optocouplers by power. Using the same method another circuit of 5 Vdc is implemented to power the buffers.

Buffers: A buffer with the reference (T54LS/T74LS244) is used; its main role is protect the STM32F4 from high current.

Optocoupler: The HCPL-3120 consists of a LED optically coupled to an integrated circuit with a power output stage. This optocoupler is ideally suited for driving power IGBTs and MOSFETs.

Resistors: Different resistors with variety of values are used.

The implemented power circuit is shown in figure 4.25 below:

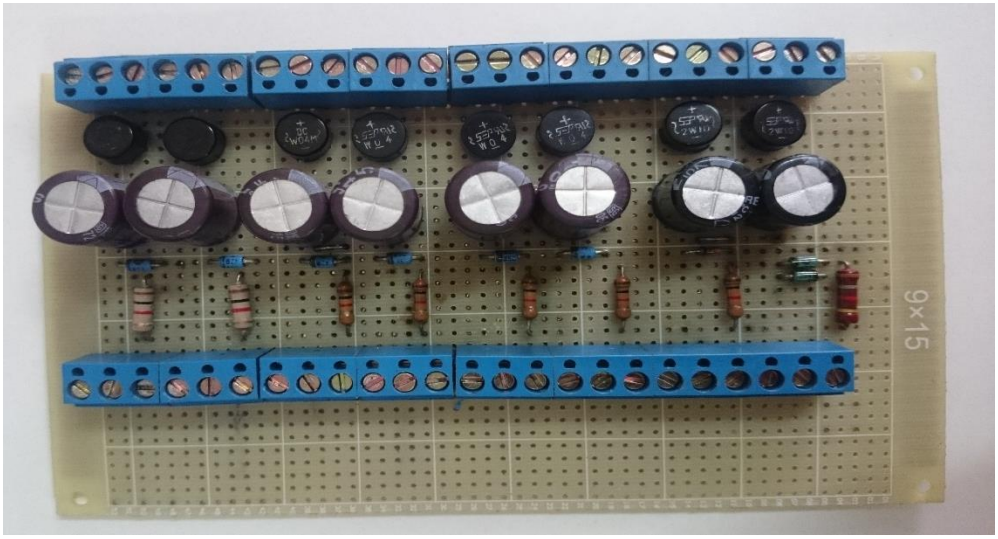

Figure 4.25 The implemented power circuit to drive the inverter IGBTs.

4.3.4 T-type inverter components

Power supplies: Two power supplies of 20V are used instead of using panels since the inverter working in open loop.

Power IGBT: A IGBT is a type of transistor used for amplifying or switching electronic signals. Twelve IGBTs with the reference of IRG4PH40KD (VCES=

1200V- VGE= 15V IC= 15A) are used in our circuit (4 for each leg), turning on/off of this IGBT's give us the desired voltage levels.

At the beginning one leg of the inverter was implemented in a breadboard (figure 4.26), after verifying its correct functionality, the three legs were printed in PCBs and connected in T-type inverter form, Figure 4.27 shows the implemented circuit.

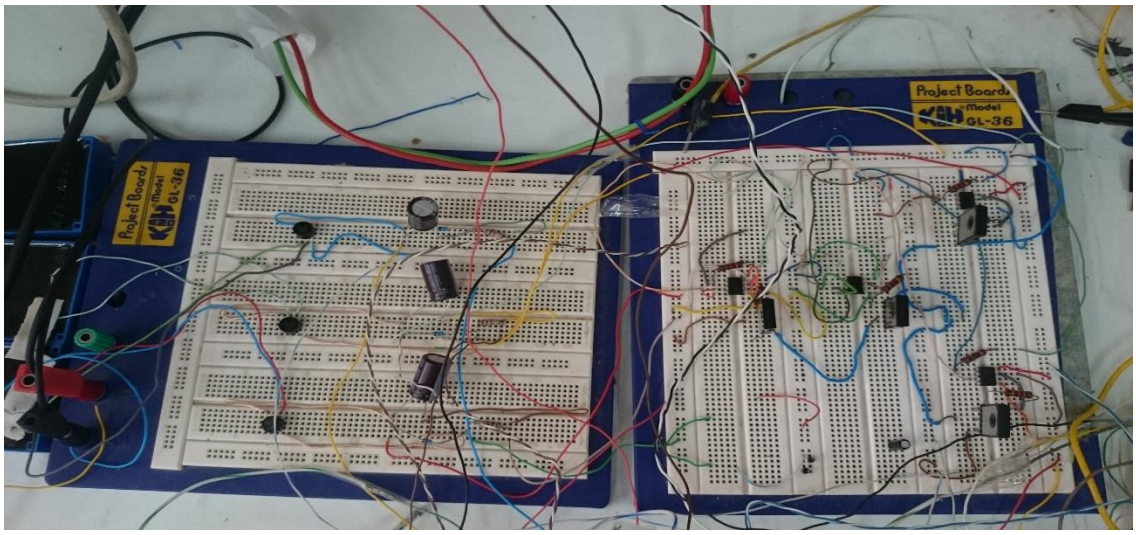

Figure 4.26 The breadboard prototype of one leg of the T-type inverter.

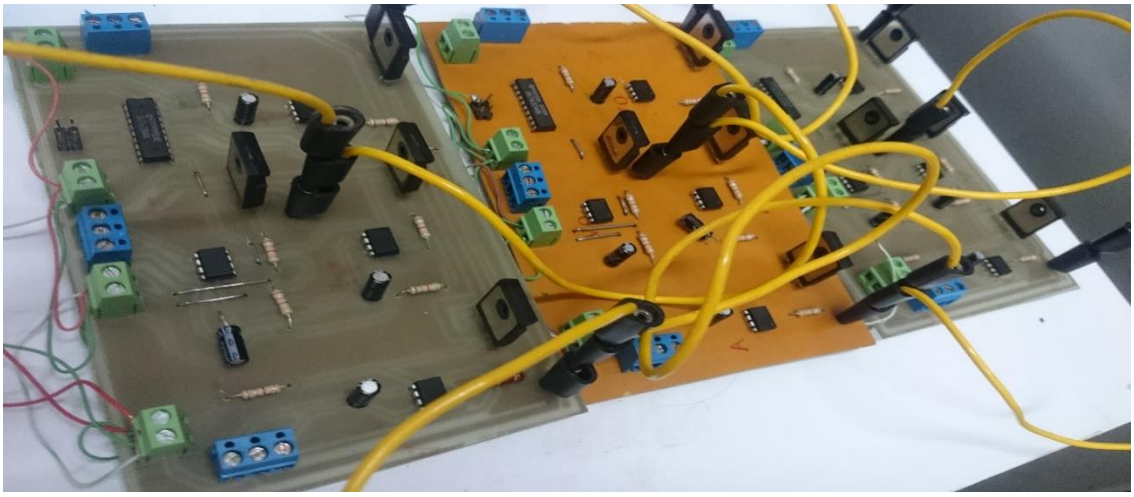

Figure 4.27 The T-type inverter designed in a PCB.

4.3.5 Experimental results

The phase to neutral voltage at the output of the inverter is shown in figure 4.28.a, whereas the line-to-line voltage wave form in shown in figure 4.28.b.

Using an LCL filter the fundamental sinusoidal AC voltage is extracted and presented in figure 4.28.c

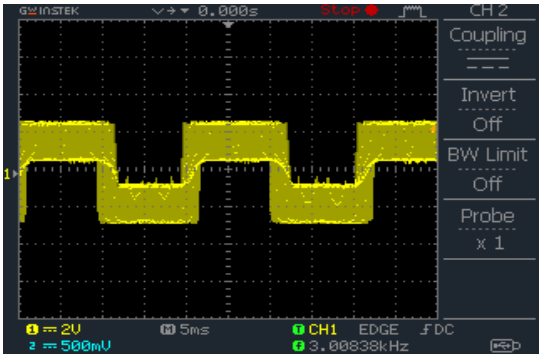

(a)

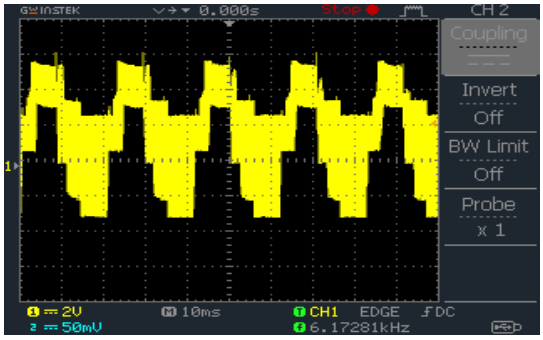

(b)

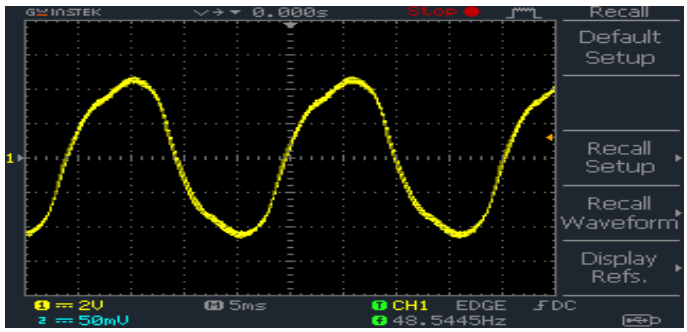

(c)

Figure 4.28 (a) The inverter line to neutral voltage, **(b)** The inverter line-to-line voltage, **(c)** The fundamental voltage waveform.

Discussion:

The phase and line voltages at the output of the T-type three level inverter are close to some extent to those obtained in the simulation, a small distortion in the line voltage is due to some problems in the stability of the transformers' output voltage.

Using the low pass LCL, the fundamental sinusoidal waveform is extracted. As it is clear in figure 4.28 the frequency of the signal is the desired 50 Hz.

4.4 Conclusion

In this chapter, three-phase three-level T-type inverter for grid connected PV system is simulated and its responsiveness was testified. The proposed system consists of PV array, T-type inverter, LCL output filter, line frequency transformer, grid utility and the proposed control strategy.

The system proved its value in terms of the system efficiency (90%) and time to reach MPP due to the use of GSS algorithm.

The T-type inverter is tested experimentally using SVM technique carried out by STM32F4 discovery kit, each element has been defined and the hardware result is discussed by the end.

General Conclusion

Throughout this work, T-type three-level inverter based single stage grid-connected PV system mathematical modeling and principal of working is presented, and a special emphasis on the key element of the PV systems that is the three-level inverter (T-type) and its controlling technique (SVM) is discussed in details.

To enhance the theoretical analysis of the system with practical results, a simulation of the system was performed using MATLAB/Simulink and the biggest part of the system that is the three-level inverter (T-type) was implemented.

For maximum power extraction from the PV system, a powerful algorithm that is the Golden section search (GSS) was used to achieve the work's goal that is extracting maximum power form the PV array, transform it into high quality AC power using LCL filter and inject it to the grid at unity power factor within the international standards.

The total system efficiency is optimized due to the low switching losses of the used inverter (T-type) and the system size and cost are reduced.

Further work

Deferent research axes can be investigated to improve further this work:

- Designing of protection system for large PV power plants such as the anti-islanding protection.
- Implementing the system with less complex and more efficient filter.
- Designing a sensorless PV system (using observers).

References

[1] Andrej Čotar, Darko Jardas, Andrej Filčić: PHOTOVOLTAIC SYSTEMS Rijeka, january 2012.

[2] Ami Shukla, Manju Khare, K N Shukla: MODELING AND SIMULATION OF SOLAR PV MODULE ON MATLAB/SIMULINK. 4, Issue 1, January 2015.

[3] Xibo Yuan: ANALYTICAL AVERAGED LOSS MODEL OF A THREE-LEVEL T-TYPE CONVERTER. Department of Electrical and Electronic Engineering, The University of Bristol, Bristol, UK, BS8 1UB. Email:xibo.yuan@bristol.ac.uk

[4] PHOTOVOLTAIC SYSTEMS. IEEE 495/695 Spring 2012.

[5] GUIDE TO INTERPRETING I-V CURVE MEASUREMENTS OF PV ARRAYS. March 1, 2011 http://www.solmetric.com

[6] Xiaodong Wang, Jianxiao Zou Jiancheng Zhao, Zhenhua Dong, Min Wei, Xie Chuan, Kai Li: COMMON-MODE VOLTAGE ELIMINATION OF THREE-LEVEL T-TYPE INVERTERS WITH A FINITE CONTROL SET MODEL PREDICTIVE CONTROL METHOD. Institute of Materials, China Academy of Engineering Physics, Mianyang, 621900, China.

[7] Mengyan Wang, Quan Chen, Guoli Li, Cungang Hu, Long Cheng, and Rui Zhou LCL Filter Design in T-Type Three-Level Grid-Connected Inverter School of Electrical Engineering and Automation, Anhui University, Hefei, China.

[8] Weixing Feng: SPACE VECTOR MODULATION FOR THREE-LEVEL NEUTRAL POINT CLAMPED INVERTER. Ontario, Canada, 2004.

[9] Mario Schweizer, Student Member, IEEE, and Johann W. Kolar, Fellow, IEEE: DESIGN AND IMPLEMENTATION OF A HIGHLY EFFICIENTTHREE-LEVEL T-TYPE CONVERTER FOR LOW-VOLTAGE APPLICATIONS.

[10] STANDARD EN 50160, VOLTAGE CHARACTERISTICS OF PUBLIC DISTRIBUTION SYSTEM, CENELEC. European Committee for Electrotechnical Standardization, Brussels, Belgium, November 1999.

[11] K.Y.Ahmed, N.Z. Yahaya, V.S. Asirvadam, K. Ramani, and O.Ibrahim: COMPARISON OF FUZZY LOGIC CONTROL AND PI CONTROL FOR A THREE-LEVEL RECTIFIER BASED ON VOLTAGE ORIENTED CONTROL. Universiti Teknologi PETRONAS Bandar Seri Iskandar, Perak 32610, Malaysia.

[12] Riad Kadri, Jean-Paul Gaubert, Member at IEEE, and Gerard Champenois, Member at IEEE: AN IMPROVED MAXIMUM POWER POINT TRACKING FOR PHOTOVOLTAIC GRID-CONNECTED INVERTER BASED ONVOLTAGE-ORIENTED CONTROL.

[13] Yao Zhezhi, Yi Lingzhi, Peng Hanmei, Fu Xi: STUDY OF SIMPLIFIED SVPWM ALGORITHM BASED ON THREE-LEVEL INVERTER. Deng Dong College of Information Engineering, Xiangtan University, 411105, China.

[14] Malu Joseph: COMPARATIVE STUDY OF MAXIMUM POWER POINT TRACKERS FOR PV SYSTEM. Nagercoil, Tamilnadu, India.

[15] FINITE-SET MODEL PREDICTIVE CONTROL AND DC-LINK CAPACITOR VOLTAGES BALANCING FOR THREE-LEVEL NPC INVERTERS. Almaktoof 2014.

[16] Akhil Nigam, Abhishek Kumar Gupta: PERFORMANCE AND SIMULATION BETWEEN CONVENTIONAL AND IMPROVED PERTURB & OBSERVE MPPT ALGORITHM FOR SOLAR PV CELL USING MATLAB/SIMULINK. IFTM University Moradabad, UP, India.

[17] Amal C Sunny, Bikram Das, P.R. Kasari, Arnab Sarkar,Sayantan Bhattacharya, Abanishwar Chakrabarty: SVPWM BASED DECOUPLED CONTROL OF ACTIVE AND REACTIVE POWER FOR SINGLE STAGE GRID CONNECTED SOLAR PV SYSTEM. NIT Agartala, India Gargi Memorial Institute of Technology, Kolkata, India.

[18] Amal C Sunny, Bikram Das, P.R. Kasari, Arnab Sarkar,Sayantan Bhattacharya, Abanishwar Chakrabarty: SVPWM BASED DECOUPLED CONTROL OF ACTIVE AND REACTIVE POWER FOR SINGLE STAGE GRID CONNECTED SOLAR PV SYSTEM. NIT Agartala, India Gargi Memorial Institute of Technology, Kolkata, India.

[19] Remus Teodorescu, Denmark Marco Liserre, Pedro Rodr´ıguez: GRID CONVERTERS FOR PHOTOVOLTAIC AND WIND POWER SYSTEMS.

[20] K.Y.Ahmed, N.Z. Yahaya, V.S. Asirvadam, K. Ramani, and O.Ibrahim: COMPARISON OF FUZZY LOGIC CONTROL AND PI CONTROL FOR A THREE-LEVEL RECTIFIER BASED ON VOLTAGE ORIENTED CONTROL. Universiti Teknologi PETRONAS Bandar Seri Iskandar, Perak 32610, Malaysia.

[21] Krunal Rao, Nil Patel: EFFECTUATION IN SPWM TECHNIQUE FOR 3-Φ VSI USING STM32F4 DISCOVERY BOARD INTERFACED WITH MATLAB. Nirma University, Ahmedabad, India.